APPLICATION OF NON-LINEAR TIME SERIES ANALYSIS TECHNIQUES TO THE NORDIC SPOT ELECTRICITY MARKET DATA

Fernanda Strozzi, Eugénio Gutiérrez Tenrreiro, Carlo Noè, Tommaso Rossi, Massimiliano Serati, José-Manuel Zaldívar Comenges

Contents

1. Introduction

The complex behaviour of financial time series, which linear stochastic models are not able to account for (Mantegna & Stanley, 2000; Johnson et al., 2003), has been attributed to the fact that financial markets are nonlinear stochastic, chaotic or a combination of both. Specifically, in the last decades there have been a considerable amount of discussion about the characterization of financial time series using the theory of Brownian motion (Osborne,1959; Malkiel, 1990), fractional Brownian motion (Mandelbrot, 1998), non-linearity (Brock *et al*., 1991), chaos and fractals (Hsieh, 1991; Lorenz, 1993; Peters, 1996), scaling behaviour (Mantegna and Stanley, 1995 and 1996), and self organized criticality (Bak and Chen, 1991; Shlesinger *et al*., 1993). The problem of characterizing financial time series is still an open question. Most of the test developed in the area of economic theory, provide evidence of nonlinear dynamics, which is a necessary but not sufficient condition for chaos. This nonlinearity may be deterministic or not deterministic. In fact, there is no convincing evidence of deterministic low-dimensionality in price series (Scheinkman and LeBaron, 1989; Papaioannou and Karytinos, 1995) and the claims of low-dimensional chaos have never been well-justified. For example, Andreadis (2000) analysing the S&P 500 index time series favours the stochastic hypothesis, whereas Friederich *et al*. (2000), using the high frequency price changes of the US dollar-German Mark support the analogy of turbulence and financial data (Mantenga and Stanley, 1996). Therefore, even though there is no conclusive evidence of low dimension deterministic (chaotic) structure, in the last few years, nonlinear time series analysis has expanded rapidly in the fields of Economics and Finance. This is also due to the fact that economic and financial time series seem to provide a promising area for the development, testing and application of nonlinear techniques (Soofi and Cao, 2002) and the fact that high frequency financial time series are readily available.

Between these time series, energy spot prices have also been analysed with several nonlinear techniques. Weron and Przybylowicz (2000) studied the electricity prices using Hurst R/S analysis and showed that they are anti-persistent with a Hurst exponent lower that 0.5. Using another technique, the Average Wavelet coefficient method, Simonsen (2003) calculated also the Hurst exponent and obtained a value of $H \approx 0.41$ in agreement also with another energy spot prices time series. In a recent study, Bask et al. (2007) estimated the Lyapunov exponents and concluded that the dynamic system that generates these prices appeared to be chaotic for the period July 1, 1999 to September 30, 2000. The question of modelling spot electricity prices has also been addressed by several researchers. Because of the high volatility in Nord Pool electricity prices, Byström (2005) applied extreme value theory (EVT) to investigate the tails of the price change distribution and then used the peaks-over-threshold (POT) method to deals with the data that exceed the threshold. Then he used a combined AR and GARCH model to fit the filtered time series to estimate as well as to forecast the time series. Along the same lines, Perelló *et al.* (2007) proposed a GARCH model for the spot price. Weron *et al*. (2004) fit a jump diffusion and regime switching model to Nordic Pool spot prices. Vehviläinen and Pyykkönen (2005) developed a stochastic factor based approach to mid-term modelling of spot prices taking into account climate data, hydro-balance, base load supply and the underlying mechanisms in spot price generation. The model was able to provide simulated values for the fundamental data, demand and supply information, and pricing strategies.

In this work we have applied non-linear time series techniques the Nordic spot electricity market data. The time series are given in two periods, from May 1992 to December 1998 and from January 1999 to January 2007. Our main interest was on trying to classify these series and analysing if their dynamical behaviour were in some way correlated with known events, e.g. the evolution of the Nord Pool and the climatic factors. This work is a first step in the direction of finding correlation of some features of the time series with the frequency and intensity of blackouts.

First, a preliminary study was carried out with the aim of characterising the time series in terms of power spectral distribution, long term memory (R/S analysis), stationarity (space-time separation plots) and tails (stable distributions). Surrogate time series were also generated to test if the original time series were similar to a stationary Gaussian linear process. In a second step, state space reconstruction parameters: time delay and embedding dimension were used to carry out the analysis of these two series in the reconstructed state space. We applied Recurrence Quantification Analysis (RQA) (Webber and Zbilut, 1994), which is based on the definition of several parameters that allows the quantification of the Recurrence Plots (RP) introduced by Eckmann *et al*. (1987). The RQA analysis of both time series has shown a certain coherent structure with a regime shift in the first time series. Moreover, the RQA analysis was repeatedly performed on 720-point epochs (approx. one month) in order to analyse the dynamic information obtained. Neighbouring epochs were shifted also by 720 points and the nonlinear variables: *%recurrence*, *%determinism, %laminarity* and *trapping time* obtained for the time series analysed. A similar analysis has also been performed with the surrogate time series. As discussed in the report, it is possible to correlate certain events with changes in *%recurrence*, *%determinism*, *%laminarity* and *trap time*. Furthermore, the RQA method allows distinguishing the original time from the surrogate the time series, indicating a certain nonlinear behaviour in the original series. The preliminary results following the analysis of these series have shown that there are some similarities in terms of certain statistical characteristics, but also differences with other high frequency financial time series (Strozzi *et al*., 2002; Strozzi *et al*., 2007). Finally, we used two RQA measures, *%determinism* and *%laminarity*, for developing a new measure of volatility which is able of detecting important historical and meteorological events with better resolution than by measuring the time series standard deviation.

2. Data provision and treatment

We have analyzed hourly data from the Nord Pool system spot prices. The series is divided into two parts. In the first part, that goes from 4th May 1992 until 31st December 1998 and comprises 58,392 data points (fig.1), the prices are indicated in Norwegian Krone (NOK)/MWh, whereas in the second time series that goes from 1st January 1999 until 26th January 2007 and comprises 70,752 data points (fig.2), the prices are expressed in EUR/MWh.

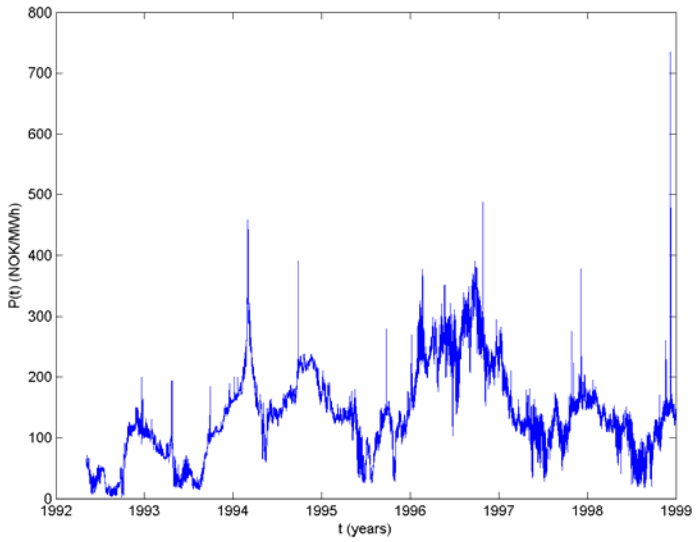

Figure 1.Spot prices in the Nordic electricity market (Nord Pool) from May 1992 until December 1998.

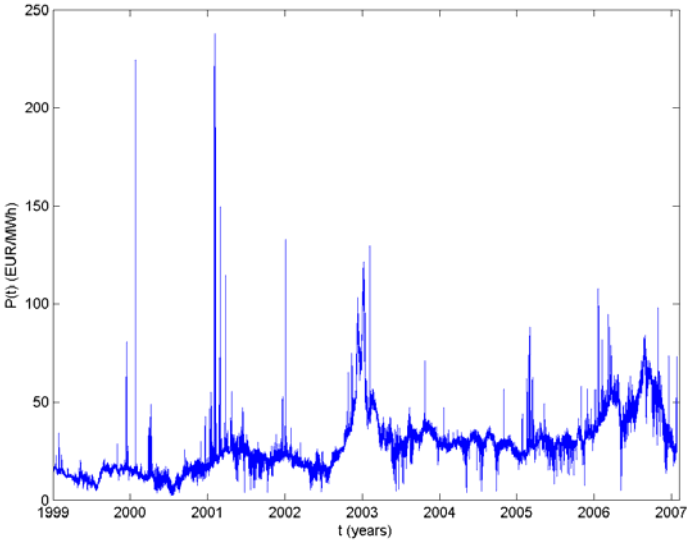

Figure 2. Spot prices in the Nordic electricity market (Nord Pool) from January 1997 until January 2007.

2.1. Data treatment

We have considered the prices time series as well as the corresponding logarithmic returns over the time horizon Δt, defined as:

$$r_{\Delta t}(t) = \ln\left(\frac{P(t)}{P(t-\Delta t)}\right) \tag{1}$$

Figures 3 and 4 show the hourly returns for the two prices time series considered.

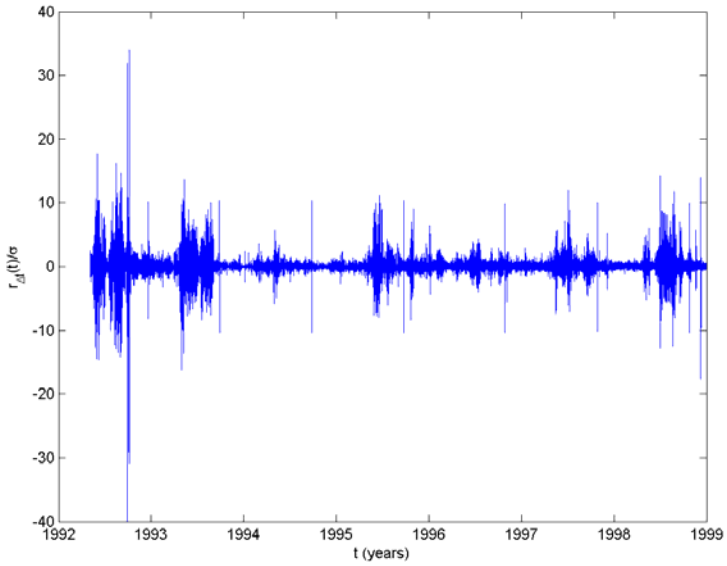

Figure 3.Hourly logarithmic return (Eq. 1) for the spot prices in the Nordic electricity market (Nord Pool) from May 1992 until December 1998.

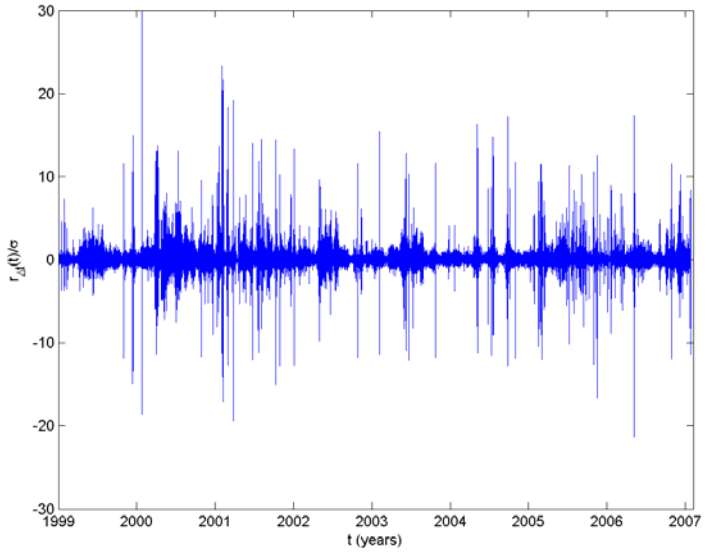

Figure 4. Hourly logarithmic return (Eq. 1) for the spot prices in the Nordic electricity market (Nord Pool) from January 1997 until January 2007.

2.2. Historical background

Electricity deregulation started in individual countries, notably United Kingdom (1990) and Norway (1991), and the Norwegian effort spread to the rest of the Nordic region before the European Union's 1996 Electricity Directive started to have real impact. This directive required that all EU countries opened up their electricity markets to competition to consumers of more than 9 GWh by 2003. The various countries are free to choose their own methods of deregulation in accordance to the criteria of the Directive. There were no provisions in the Directive for a power pool or the establishment of financial markets (Mork, 2001). The Nordic electricity market, known as Nord Pool (http://www.nordpool.no) was created in 1993 and it is owned by the two national grid companies, Statnett SF in Norway (50%) and Affärverket Svensa Kraftnät in Sweden (50%). It was

established as a consequence of the decision in 1991 by the Norwegian Parliament's to deregulate the market for power trading.

Therefore, between 1992 and 1995 only Norway contributed to the market, in 1996 a joint Norwegian-Swedish power exchange was started-up and the power exchange was renamed Nod Pool ASA. Finland started a power exchange market of its own, EL-EX, in 1996, and joined Nord Pool in 1997. Beginning of 15th June 1998, Finland became an independent price area on the Nord Pool Exchange. The western part of Denmark (Jutland and Funen) has been part of the Nordic electric power market since 1 July 1999, whereas the eastern part of Denmark entered after 1st October 2000. On 5th October 2005 also the German area KONTEK was added in the Nord Pool exchange market. Table 1 summarises the historical evolution of the Nord Pool, whereas in Table 2 the deregulation process is also indicated.

Table 1. Nord Pool participating countries and dates of entry.

Countries	**Date of entry of new country (dd/mm/yy)**
Norway	1/1/93
Norway and Sweden	1/1/96
Norway, Sweden and Finland	29/12/97
Norway, Sweden, Finland and western Denmark	1/7/99
Norway, Sweden, Finland, western and eastern Denmark	1/10/00
KONTEK (Germany)	5/10/05

Table 2. Summary of the deregulation process in Nord Pool members.

	1991	**1992**	**1993**	**1994**	**1995**	**1996**	**1997**	**1998**	**1999**	**2000**	**2001**	**2002**	**2005**	**2004**	**2005**
Norway															
Sweden															
Finland															
West Denmark															
East Denmark															
Kontek															

green= deregulation process; blue= NordPool member

The new bidding area named KT offered geographic access to the Vattenfall Europe Transmission control area from East Denmark and allowed Nord Pool to compete directly with European Energy Exchange (EEX). Kontek cable connects Zealand and Germany. Nord Pool owns 17.39% of the shares of EEX and proposed a common market with EEX, but EEX did not agree (Kristiansen, 2006; 2007). Nevertheless the existence of a common electricity market, there are still national transmission system operators and some differences with respect to transmission pricing.

The spot market operated by Nord Pool is an exchange market where participants' trade power contracts for physical delivery the next day and is thus referred to as a day-ahead market. The spot market is based on an auction with bids for purchase and sale of power contracts of 1-h duration covering the 24 h of the following day. At the deadline for the collection of all buy and sell orders the information is gathered into aggregate supply and demand curves for each power-delivery hour. From these supply and demand curves the equilibrium spot prices-referred to as the system prices-are calculated.

When no grid congestion exists there will be a single identical price across the area with no congestions. However, when there is insufficient transmission capacity in a sector of the grid, grid congestion will arise and the market system will establish different "price areas". This is because the Nordic market is partitioned into separate bidding areas which become separate price areas when the contractual flow between bidding areas exceeds the capacity allocated by the transmission system operators for spot contracts. In the case of congestion the transmission system operators ask generators to reduce (increase) production or large buyer to increase (decrease) demand until excess of supply or demand are eliminated. The fact that separate prices may coexist depending upon regional supply and demand causes the relevant market definition to vary with time. Sometimes the prices are of the entire Nordic region. Sometimes more than one price area exists (Haldrup and Nielsen, 2006). Thus, whenever the relevant interconnector capacity is insufficient the Nord Pool area is divided into two or several "price areas". Sweden is always one single price area, and the same applies to Finland. In Denmark the transmission system is divided into two parts, West and East, and consequently there are two price areas. In Norway the congestion charges effectively divides the country into five price areas. In addition to the "area prices" there is a "system price". This price is determined under the assumption that no transmission constraint is binding. The system price is the reference price in the financial contracts (Amundsen and Bergman, 2007). Haldrup and Nielsen (2006) found that looking to hourly data from 3.1.2000 to 25.10.2003, 34.24% of time all the prices for the entire Nordic region where identical. Two price areas existed in 34.55% and three in 20.86 % of the time. In only 11 hours there was complete congestion and six different price areas existed i.e. one for each geographical market. Despite these differences, in this work we will only consider "system price".

The variation of the prices in the Nord pool system is well correlated with the variations in precipitation in Norway and Sweden because of its strong dependence of the hydropower generation. Table 3 summarises the climatic conditions during the last years. The 1996 was a "dry" year, while 1997-2000 was a series of "wet" years. The 2000 was not very "wet" and the first part of 2001 was quite "dry" but the autumn was very rainy and 2001 started well with a water reservoir above the normal. Very special hydrological conditions appeared during the autumn and winter season of 2002-2003 with a sharp decline of precipitation. This was a rare event that could happen only every 100-200 years (Weron *et al*., 2004). The result was the increasing of spot prices in 2003.

Table 3. Summary of meteorological conditions: Dry and wet years.

year	***state***	***Period considered***
1996	dry	1.1.96-31.12.96
1997-2000	wet	1.1.97-31.12.99
2000	not very wet	1.1.2000-31.12.2000
First part 2001	dry	1.1.2001-31.8.2001
Autumn 2001	very wet	1.9.2001-31.12.2001
2002-2003	very dry (rare event)	1.1.2002-31.12.2003

By looking into figs. 1-2 and comparing with Table 3, we can observe these correlations in the electricity price. However, weather conditions are not able to explain all the features in the time series. For example, the relative sharp price increase between 2000 and 2001 could be explained by a combination of the market power exercised by the mayor generators, the increased demand and higher fuel prices (Weron *et al.*, 2004). Moreover spot prices can increase tenfold during a single hour. Jumps in the spot prices are an effect of extreme load fluctuations, caused by severe weather conditions often in combination with generation outages or transmission failures. These spikes are normally quite short lived, and as soon as the weather phenomenon or outage is over, prices fall back to a normal level. Jumps tend to be more severe during high price periods and a positive jump may be followed by a negative jump to capture the rapid decline of electricity prices (Weron *et al*., 2004).

2.3. Material and methods

There are different freely available software packages on the Internet that may be used to perform non-linear time series analysis. In this work, we have used several of them for different purposes as indicated bellow.

One of the most complete is the TISEAN software package (http://www.mpipks-dresden.mpg.de/~tisean) which has incorporated an impressive quantity of algorithms developed in the nonlinear time series analysis field (Kantz and Schreiber, 1997). There is a version for MATLAB® users developed at Göttingen University, called TSTOOL, that can be download at http://www.physik3.gwdg.de/tstool/. Furthermore, a commercially available software package developed by Abarbanel and co-workers (Abarbanel, 1996) and commercialised by Randle Inc., called Csp, can be found at http://www.chaotic.com/.

Concerning Recurrence Quantification Analysis, the original programs developed by Weber and Zbilut (1994) can be download at at http://homepages.luc.edu/~cwebber., whereas a MATLAB® version of RQA developed at the University of Postdam called CRP toolbox can be found at http://tocsy.agnld.uni-postdam.de (Marwan *et al*., 2007). In addition, there is a commercially available version called VRA (Visual Recurrence Analysis) that can be obtained at http://home.netcom.com/~eugenek/download.html

Finally, the analysis of stable distributions has been carried out using the program STABLE for univariate data (http://www.cas.american.edu/~jpnolan).

3. Embedding theory

The mathematical basis of continuous dynamical modelling is formed by differential equations of the following type:

$$\frac{d\mathbf{x}}{dt} = \mathbf{F}(\mathbf{x}, \alpha) \tag{2}$$

where the real variable t denotes time, $\boldsymbol{x} = (x_1, x_2, \ldots, x_n)$ represents the state variables of the system, depending on time t and on the initial conditions, and α_j are parameters of the system, while $\boldsymbol{F} = (F_1, F_2, \ldots, F_n)$ is a nonlinear function of these variables and parameters. Actual states of these systems are described by the vector variable $\boldsymbol{x}$ consisting of n independent components. Each state of the system corresponds to a definite point in phase space, which is called phase point. The time variation of the state of the system is represented as a motion along some curve called phase trajectory.

Experimentally, it is not always possible to measure the complete state of a system and, normally, when analysing a dynamical system, we have access to few observable quantities which, in the absence of noise, are related to the state space coordinates by:

$$s(t) = \mathbf{h}(\mathbf{x}(t)) \tag{3}$$

where $\boldsymbol{h}$ is normally an unknown nonlinear function called measurement function. The theory of embedding is a way to move from a temporal time series of measurements to a state space "similar" -in a topological sense- to that of the underlying dynamical system we are interested in analysing. Techniques of state space reconstruction were introduced by Packard *et al.* (1981) and Takens (1981), which showed that it is possible to address this problem using measurements of a sufficient long time series, $s(t)$, of the dynamical system of interest. Takens proved that, under certain conditions, the dynamics on the attractor of the underlying original system has a one-to-one correspondence with measurements of a limited number of variables. This observation opened a new field of research. In fact, if the equations defining the underlying dynamical system are not known, and we are not able to measure all the state space variables, the state space of the original system is not directly accessible to us. However, if by measuring few variables we are able to reconstruct a one-to-one correspondence between the reconstructed state space and the original, this means that it is possible to identify unambiguously the original state space from measurements. Embedding theory has opened a new field of research: nonlinear time series analysis (Tong, 1990; Abarbanel, 1996; Kantz and Schreiber, 1997; Diks, 1999, amongst others).

In order to explain the relationship that occurs between the reconstructed and the real state space, let us consider the following dynamical system

$$\frac{d\mathbf{x}}{dt} = \mathbf{F}(\mathbf{x}); \quad \mathbf{x} = (x_1, x_2, x_3) \tag{4}$$

We can define $\mathbf{y} = (y_1, y_2, y_3)$ as follows: $\mathbf{y} = (x_1, dx_1/dt, d^2x_1/dt^2)$, then the equations of motion take the form

$$\frac{dy_1}{dt} = y_2$$

$$\frac{dy_2}{dt} = y_3 \qquad (5)$$

$$\frac{dy_3}{dt} = \mathbf{G}(y_1, y_2, y_3)$$

for some function **G**. In this coordinate system, modelling the dynamics reduces to constructing the single function **G** of three variables, rather than three separate functions, each of three variables.

In this way we may proceed from the state space (x_1, x_2, x_3) to the space of derivatives $(x_1, dx_1/dt, d^2x_1/dt^2)$. The dynamics in this new space will be related to the dynamics of the original space by a nonlinear transformation which is called the reconstruction map. The extension of this approach to higher-dimensional dynamical systems is straightforward by considering higher derivatives.

The advantage in considering the space of derivatives is that we can approximate them from measurements of x_1. But what kind of information about the original space is preserved in the new one?

There are two types of preserved information: qualitative and quantitative. Qualitative information is that which allows a qualitative description of the dynamics described by topological invariants, such as for instance, singularity of the field, closeness of an orbit, stability of a fixed point, etc. (Gilmore, 1998) Quantitative information can be of two different types: geometrical and dynamical. Geometrical properties (Grassberger, 1983) consist on fractal dimensions or scaling functions. Dynamical methods (Wolf *et al*., 1985) rely on the estimation of local and global Lyapunov exponents and Lyapunov dimensions. In order to guarantee that the quantities computed for the reconstructed attractor are identical to those in the original state space, we require that the structure of the tangent space, i.e. the linearization of the dynamics at any point in the state space, is preserved by the reconstruction process. The problem is to see under what conditions this can happen. Embedding theorems try to shed some light on this problem.

Let *s(t)* be the measure of some variable of our system, see Eq. (3). Takens (1981) shown that instead of derivatives, $\{s(t), \dot{s}(t), \ddot{s}(t), ...\}$, one can use delay coordinates, $\{s(t), s(t+\Delta t), s(t+2\Delta t), ...\}$, where Δt is a suitably chosen time delay. In fact, looking at the following approximation of the derivative of *s(t)*:

$$\frac{ds(t)}{dt} \cong \frac{s(t+\Delta t) - s(t)}{\Delta t} \qquad (6)$$

$$\frac{d^2s(t)}{dt^2} \cong \frac{s(t+2\Delta t) - 2s(t+\Delta t) + s(t)}{2\Delta t^2} \qquad (7)$$

it is clear that the new information brought from every new derivative is contained in the series of the delay coordinates. The advantage of using delay coordinates instead of derivatives is that in case of high dimensions high order derivatives will tend to amplify considerably the noise in the measurements.

Another generally used method, for state space reconstruction, is singular value decomposition (SVD), otherwise known as Karhunen-Loève decomposition, which was proposed by Broomhead and King (1986) in this context. The simplest way to implement this procedure is to compute the covariance matrix of the signal with itself and then to compute the eigenvalues, i.e. if *s(t)* is the signal at time *t*, the elements of the covariance matrix **Cov** are:

$$c_{ij} = \left\langle s(t)s(t+(i-j)t)\right\rangle^{T} \quad (8)$$

where i and j go from 1 to n where n is bigger or equal to the dimension of the system in this new space. The eigenvectors of **Cov** define a new coordinate system. Typically, one calculates the dimension of the reconstructed phase space by considering only eigenvectors whose eigenvalues are "large".

Then, from the space of derivatives, time lags or eigenvectors, it is possible to extract information about the underlying system, which was generating the measured data.

In order to preserve the structure of tangent space and then the dynamic characteristic of it, the relation between the reconstructed space and the original one has to be an embedding of a compact smooth manifold into R^{2n+1}, which means a one-to-one immersion i.e. a one-to-one C^1 map with Jacobian which has full rank everywhere. The point now is to show under what conditions the reconstruction forms an embedding.

A general existence theorem for embedding in Euclidean spaces was given by Whitney (1936) who proved that a smooth (C^2) n-dimensional manifold may be embedded in R^{2n+1}. This theorem is the basis of the time delay reconstruction (or embedding) techniques for phase space portraits from time series measurements proposed by Takens (1981), who proved that, under certain circumstances, if d_E -the dimension of the reconstructed state vector, normally called the embedding dimension- is greater or equal to $2n+1$, where n is the dimension of the original state space, then the reconstructed states fill out a reconstructed state space which is diffeomorphic, i.e. a one-to-one differentiable mapping with a differentiable inverse, to the original system. Generally speaking, the embedding dimension is the minimal number of dynamical variables with which we can describe the attractor when we know only one of its state variables or a function related to them.

Apart from the methods mentioned above, there are several other methods of reconstructing state space from the observed quantity $s(t)$ that have appeared in the literature -for a critical review see Breeden and Packard (1994). Although the method of reconstruction can make a big difference in the quality of the resulting coordinates, it is not clear in general which method is the best. The lack of a unique solution for all cases is due in part to the presence of noise and to the finite length of the available data sets.

For Takens' theorem to be valid we need to assume that the underlying dynamics is deterministic and that both the dynamics and the observations are autonomous, i.e. **F** and **h** in Eqs. (2) and (3) depend only on $\boldsymbol{x}$ and not on t. Unfortunately, this is not the case of many systems in the field of control and communications which are designed to process some arbitrary input and hence, cannot be treated as autonomous. The extension of Takens' theorem to deterministically forced stochastic systems has been recently developed by Stark *et al.* (1997). In particular they proved that such an extension is possible for deterministically forced systems even when the forcing function is unknown, for input-output systems (which are just deterministic systems forced by an arbitrary input sequence) and for irregular sampled systems.

Another problem in embedding theory is that Takens' theorem has been proven for noise-free systems. Unfortunately, there is always a certain amount of noise, $\sigma(t)$, in real data. Such noise can appear in both the measurements and the dynamics (Diks, 1999). Observational noise, i.e. $s(t)=h(\mathbf{x}(t))+\sigma(t)$, does not affect the evolution of the dynamical system, whereas dynamical noise acts directly on the state of the dynamical system influencing its evolution, for example: $d\mathbf{x}/dt=\mathbf{F}(\mathbf{x},\alpha)+\sigma(t)$.

The effects of relatively small amount of observational noise may put severe restrictions on the characterisation and estimation of the properties of the underlying dynamical system. In order to remove the observational noise different possibilities are available which can be broadly divided into two categories: linear filters (Badii *et al*., 1988) and special nonlinear noise reduction methods that make use of the deterministic origin of the signal we are interested in (for a recent survey see: Kostelich and Schreiber, 1993; Davies, 1994). However, in the case of dynamical noise, the reconstruction theorem does not apply and it may even be impossible to reconstruct the state of the system (Takens, 1996). In this situation, systems must be examined case by case before analysis. In particular, Stark *et al*. (1997) showed that the extension of Takens' theorem is possible for deterministic systems driven by some stochastic process.

3.1. Embedding parameters

The embedding theorem is important because it gives a rigorous justification for the state space reconstruction. However, Takens' theorem is true for the unrealistic case of an infinite, noise-free, number of points. Takens showed that, in this case, the choice of the time delay is not relevant, and gave indications only on the choice of the embedding dimension.

Nevertheless, in real applications, the proper choice of the time delay τ and the calculation of an embedding dimension, d_E, are fundamental for starting to analyse the data. As a matter of fact, a lot of research on state space reconstruction has centred on the problems of choosing the time delay and the embedding dimension which we can call the parameters of the reconstruction for delay coordinates.

If the time delay chosen is too small, there is almost no difference between the elements of the delay vectors, since that all points are accumulated around the bisectrix of the embedding space: this is called redundancy (Casdagli *et al*., 1991). However, when τ is very large, the different co-ordinates may be almost uncorrelated. In this case the reconstructed trajectory may become very complicated, even if the underlying "true" trajectory is simple: this is called irrelevance. Unfortunately no rigorous way exists of determining the optimal value of τ. Moreover, similar problems are encountered for the embedding dimension. Working in a dimension larger than the minimum required by the data will lead to excessive requirements in terms of the number of data points and computation times necessary when investigating different questions such as, for example invariants calculation, prediction, etc. Furthermore, noise by definition has an infinite embedding dimension, so it will tend to occupy the additional dimensions of the embedding space where no real dynamics is operating and, hence, it will increase the error in the subsequent calculations. On the other hand, by selecting an embedding dimension lower than required, we would not be able to unfold the underlying dynamics, i.e. the calculations would be wrong since we do not have an embedding.

When derivatives, $\{s(t), \dot{s}(t), \ddot{s}(t), ...\}$, or SVD are employed there is no need to determine an optimum time delay. Nevertheless, for the case of derivatives, the reconstruction will depend on the way they are numerically calculated (which turns out to depend on different parameters, see for example (Burden and Faires, 1996) for a review of numerical calculation of derivatives). In practice for each method we will carry out a slightly different state space reconstruction. For the case of SVD, the time delay chosen is unitary, but there is still the problem of choosing the time scale or window in which the calculations are performed. Broomhead and

King (1986) in fact, concluded that the effects of window length should be carefully investigated each time a state space reconstruction is carried out.

4. Chaotic time series analysis

Nonlinear analysis of experimental time series has, among its goals, the separation of high-dimensional and stochastic dynamics from low-dimensional deterministic signals, estimation of system parameters or invariants (characterisation), and, finally, prediction, modelling and control.

Unfortunately it seems very difficult to tell whether a series is stochastic or deterministically chaotic or some combination of these categories. More generally, the extent to which a non-linear deterministic process retains its properties when corrupted by noise is also unclear. The noise can affect a system in different way, either in an additive way or as a measurement error, even though the equations of the system remain deterministic.

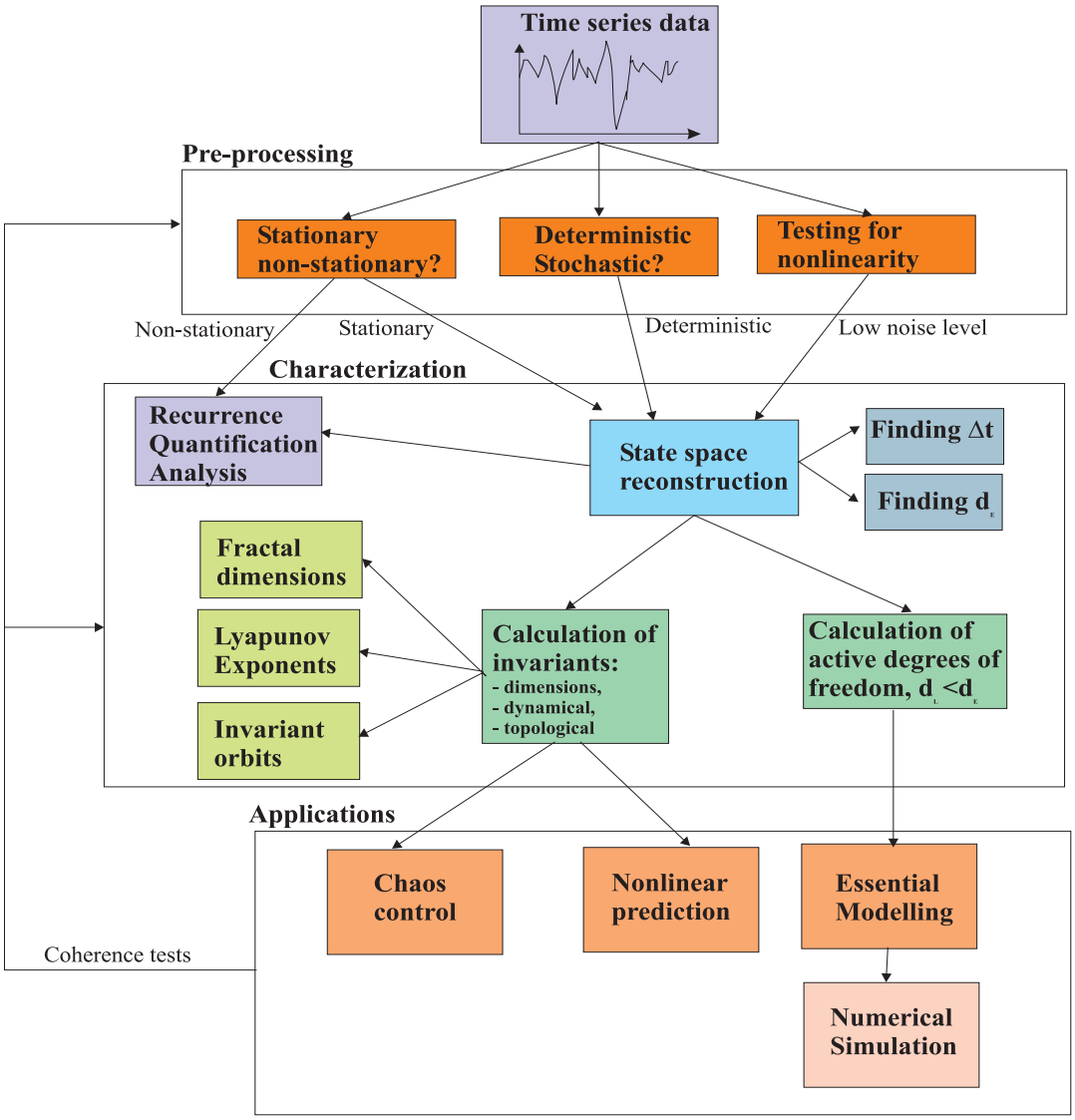

Figure 5. Schematic representation of nonlinear time series analysis using delay coordinate embedding (Strozzi and Zaldívar, 2002).

A schematic representation of the different steps is given in Fig. 5. Since a single reliable statistical test for chaoticity is not available, combining multiple tests is a crucial aspect, specially when one is dealing with limited and noisy data sets like in economic and financial time series.

There are different aspects that should be carefully studied before attempting to go further using nonlinear time series analysis methods. A long and exhaustive discussion can be found in Schreiber (1998) and the basic methodologies will be presented during the analysis part. Here, we are briefly going to indicate the main problems one should be aware of. These can be summarized as follows:

- has the phenomenon been sufficiently sampled?;
- is the data set stationary or can one remove the nonstationary part?;
- is the level of noise sufficiently low so that one can obtain useful information using nonlinear time series techniques?

Some tests to study these questions have been recently implemented in the TISEAN software package (Hegger *et al*., 1999), which has incorporated a substantial quantity of algorithms developed for nonlinear time series analysis.

The problem of the number of samples needed to carry out state space reconstruction is related to the dimensionality of the problem we are dealing with. In order to characterize properly the underlying dynamics from the observed time series, we need to sample properly the phase space in which our dynamical system lies. As the dimension of the underlying system increases, a higher number of samples is needed. Ruelle (1990) discussed this problem, and based on simple geometrical considerations, he arrived at the following conclusion: if the calculated dimension of our system is well below $2log_{10}m$, where m is the total number of points in the original time series, then we are using a sufficient number of data points. Of course having a sufficient number of data points is a necessary but not a sufficient condition for reliable nonlinear time series analysis.

Another related problem is the sampling rate. Consider the case when we are sampling data from a, presumably, chaotic system. Chaotic systems, like stochastic ones, are unpredictable in the long run. This long run is related to the speed at which nearby trajectories diverge in phase space, which turns out to be related to the Lyapunov exponents of the system under study. Hence, if we are sampling at a rate slower than our predictability window, even though the underlying system is chaotic, we will find that our system behaves as a stochastic one. In this situation, if one suspects that the underlying system is deterministic, the best thing to do is to repeat the experiment by increasing the sampling rate. Interpolating between data points would be of no use as no new information is introduced.

A time series is said to be strictly stationary if its statistical distribution does not change across time. More specifically, suppose we have a set of m samples of the series $s(t)$ made at times t_1 through t_m, these need not be contiguous times. Strict stationarity implies that the joint probability density function of those m samples is identical to the joint probability distribution of another m samples taken at times t_{1+k} through t_{m+k}. This must be true for all the choices of m and k, as well for the m relative sample times. Why is stationarity so important? Because almost all methods developed by linear and nonlinear time series analysis assume that the time series we are analysing is stationary, which implies that the parameters of the system that has generated the time series, remain constant. For this reason time-series analysis often requires one to turn a nonstationary series into a stationary one so as to use these theories. Unfortunately, nonstationary signals are very common in particular

when observing natural or man-made phenomena, and in some cases the nonstationary components, such as the trend, may sometimes be of more interest than that of the stationary part obtained by removing the trend or the seasonal variation from the signal.

Even though a precise definition of stationarity exists, there is no magic formula for deciding whether a series is stationary or not. However, strong violations of the basic requirements that the dynamical properties of the system must not change, beyond their statistical fluctuations, can be checked simply by measuring such properties, i.e. mean, variance, spectral components, correlations, etc., for several segments of the data set. Nonlinear time series analysis has also developed its own techniques to study nonstationarity as we will see bellow.

4.1. Preliminary Analysis

4.1.1. Surrogate time series generation

If the dynamics that has generated the time series is not known or if the data are noisy, it is important to investigate whether the amount of nonlinear deterministic dependencies is worth analyzing further or whether the series can be considered as stochastic. Hence, one of the first steps before applying nonlinear techniques to the Nord Pool data is to investigate if the use of such advanced techniques is justified by the data. The main reason behind this reasoning is that linear stochastic processes can create very complicated looking signals and that not all the structures that we find in a data set are likely to be due to nonlinear dynamics going on within the system. The method of surrogate data, see for example Schreiber and Schmitz (2000) for a review, has become a useful tool to address the question if the irregularity of the data is most likely due to nonlinear deterministic structure or rather due to random inputs to the system or fluctuations in the parameters.

The method of surrogate data, which was first introduced by Theiler *et al.* (1992) in nonlinear time series analysis, consists of generating an ensemble of "surrogate" data sets similar to the original time series, but consistent with the null hypothesis, usually that the data have been created by a stationary Gaussian linear process, and of computing a discriminating statistic for the original and for each of the surrogate data sets

In general a linear stochastic process can be described by

$$x_n = a_0 + \sum_{i=1}^{M_1} a_i x_{n-i} + \sum_{j=1}^{M_2} b_j \eta_{n-j} \qquad (9)$$

where η_n are independent Gaussian random numbers with zero mean and unit variance and a_i, b_i, M_1 and M_2 are constants. This is called an ARMA(M_1, M_2) process. Now we want to test the hypothesis that the data could be explained by a linear model. A statistical significance test consists on the following steps: a/ we compute some nonlinear observable λ_0 from the data; b/ we observe if the value obtained suggests that the data are nonlinear and we calculate the same quantity from a number of comparable linear models. If the results are completely different the data might be nonlinear. If we have any theory for the distribution of the values of λ_i for linear stochastic process, we can estimate their distribution using the method of *surrogate data*. The null hypothesis that we want to test is that the data results from a Gaussian linear stochastic process. Then we should specify the *level of significance*. If we allow for a 5% chance that we reject the null hypothesis although

it is in fact true (valid at a 95% significance level) then more than one wrong result out of 19 is usually not considered acceptable (Schreiber and Schmitz, 2000). How to make surrogate data sets? Let we suppose that the data came from a stationary linear stochastic process with Gaussian inputs. We consider the mean, the variance and the autocorrelation function of the real data or equivalently the mean and the power spectrum.

We can create surrogate data by taking their fast (discrete) Fourier transform (FFT) and multiplying it by a random phase parameter uniformly distributed in [0,2π[, then it is possible to compute the inverse of FFT and we have a time series with the prescribed spectrum. Different realization of the random phase gives new surrogate data. This process of phase randomisation preserves the Gaussian distribution.

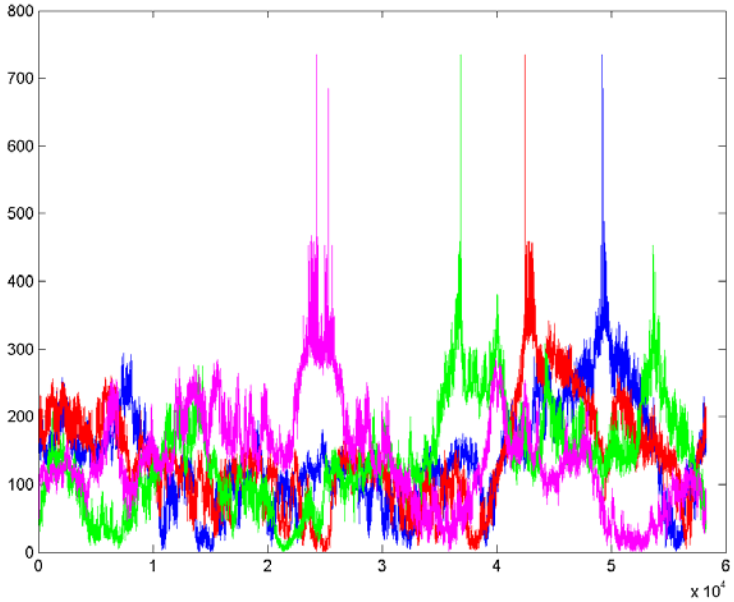

Figure 6. Four surrogate time series generated for the Nord pool spot price in Norwegian Krone (Fig. 1) using the TISEAN software package (Hegger *et al*., 1999) with *surrogates* program.

In this work, we have created 19 surrogate data sets (same mean, variance and Fourier power spectrum) for each Nord Pool spot prices time series, for example see Fig. 6, these time series data comes from a stationary linear stochastic process with Gaussian inputs.

In addition, we have also considered another null hypothesis: the data are simply *temporally uncorrelated noise* i.e. the null hypothesis is any correlation at all. Surrogate data in this case are generated by a random shuffling of the original time series. Also, in this case, we have created 19 surrogate data sets from the original time series.

4.1.2. R/S Analysis

A tool for studying long-term memory and fractality of a time series is the Rescaled Range analysis (R/S analysis) first introduced by Hurst (1951) in hydrology. Mandelbrot (1983) argued that R/S analysis is a more powerful tool in detecting long range dependence when compared to more conventional analysis like autocorrelation analysis, variance ratios and spectral analysis. In this method, one measures how the range of cumulative deviations from the mean of the series is changing with the time. It has been found that, for some time series, the dependence of R/S on the number of data points (or time) follows an empirical power law

described as $(R/S)_n=(R/S)_0\, n^H$, where $(R/S)_0$ is a constant, n is the time index for periods of different length, and H is the Hurst exponent. $(R/S)_n$ is defined as

$$\left(\frac{R}{S}\right)_n = \frac{\max_{1\le t\le n} A(t,n) - \min_{1\le t\le n} A(t,n)}{\sqrt{\frac{1}{n}\sum_{t=1}^{\tau}(s(t)-\langle s\rangle_n)^2}} \tag{10}$$

where $A(t,n)$ is the accumulated departure of the time series $s(t)$ from the time average over the time interval n: $\langle s\rangle_n$ $A(t,n)=\sum_{i=t}^{t+n}(s(i)-\langle s\rangle_n)$.

The Hurst exponent, $0\le H\le 1$, is equal to 0.5 for random walk time series, <0.5 for anticorrelated series, and >0.5 for positively correlated series. The Hurst exponent is directly related to the "fractal dimension", which gives a measure of the roughness of a surface. The relationship between the fractal dimension, D, and the Hurst exponent, H, is:

$$D = 2 - H \tag{11}$$

Hurst exponents quantify the correlation of a fractional Brownian motion. A fractional Brownian motion (fBm) is a random walk with a Hurst exponent different from 0.5 and then with a memory. The decaying of spectral density of a fBm has a relationship with the Hurst exponent as follow:

$$spectral\ density \propto \frac{1}{f^{\alpha}} \tag{12}$$

where $\alpha = 2H + 1$.

Financial time series have been found to exhibit some universal characteristics that resemble the scaling laws typical of natural systems in which large numbers of units interact. For instance, the Hurst exponent has been extensively applied by Peters (1996) to various capital markets and in most of the cases he has found persistent memory.

A long memory process is a process with a random component, where a past event has a decaying effect on future events. The process has some memory of past events, which is "forgotten" as time moves forward. The mathematical definition of long memory processes is given in terms of autocorrelation. When a data set exhibits autocorrelation, a value x_i at time t_i is correlated with a value x_{i+d} at time t_{i+d}, where d is some time increment in the future. In a long memory process autocorrelation decays over time and the decay follows a power law, i.e

$$p(k) = Ck^{-\beta} \tag{13}$$

where, C is a constant and $p(k)$ is the autocorrelation function with lag k. The Hurst exponent is related to the exponent β by

$$H = 1 - \frac{\beta}{2} \tag{14}$$

In this work we have used the standard scaled windowed variance method (Cannon *et al.*, 1997) to estimate H by linear regression of $log(R/S)$ versus $log(Windowsize)$. The results for the two original time series and the surrogate series are shown in Tables 4-5. As it can be seen both time series show antipersistence, $H<0.5$. This

has already been found by several researchers (Weron and Przybylowicz, 2000; Simonsen 2003; Perelló *et al.* 2007, amongst others).In all cases, the Hurst exponents of the original time series are slightly higher than those of the linear surrogate time series but this does not mean that the value of *H* helps us to distinguish between the original time series and their surrogates, because H for the linear surrogate of NOK is higher than H for real EUR (Table 4). For the shuffled surrogate time series we can observe that H for surrogates is nearer to 0.5 independently if we consider the surrogate of NOK or of EUR (Table 5).

Table 4. Hurst exponents for the Nord pool and the surrogate linearly correlated time series.

Data set	H	Data set	H
NOK	0.4406	*EUR*	0.2673
Surr01_nl	0.3632	*Surr01_el*	0.1231
Surr02_nl	0.3824	*Surr02_el*	0.0899
Surr03_nl	0.3399	*Surr03_el*	0.1402
Surr04_nl	0.3646	*Surr04_el*	0.1631
Surr05_nl	0.3276	*Surr05_el*	0.1597
Surr06_nl	0.4151	*Surr06_el*	0.1325
Surr07_nl	0.3480	*Surr07_el*	0.0914
Surr08_nl	0.3497	*Surr08_el*	0.2262
Surr09n_l	0.3125	*Surr09_el*	0.1063
Surr10_nl	0.3024	*Surr10_el*	0.1673
Surr11_nl	0.3396	*Surr11_el*	0.1434
Surr12_nl	0.3624	*Surr12_el*	0.1612
Surr13_nl	0.3795	*Surr13_el*	0.1990
Surr14_nl	0.3602	*Surr14_el*	0.1604
Surr15_nl	0.3574	*Surr15_el*	0.1368
Surr16_nl	0.3406	*Surr16_el*	0.2096
Surr17_nl	0.3874	*Surr17_el*	0.1814
Surr18_nl	0.3369	*Surr18_el*	0.1089
Surr19_nl	0.3774	*Surr19_el*	0.0905

Table 5. Hurst exponents for the Nord pool and the surrogate shuffled time series.

Data set	H	Data set	H
NOK	0.4406	*EUR*	0.2673
Surr01_ns	0.4886	*Surr01_es*	0.4293
Surr02_ns	0.4842	*Surr02_es*	0.4293
Surr03_ns	0.4847	*Surr03_es*	0.4423
Surr04_ns	0.4773	*Surr04_es*	0.4136
Surr05_ns	0.4857	*Surr05_es*	0.4267
Surr06_ns	0.5036	*Surr06_es*	0.4437
Surr07_ns	0.4877	*Surr07_es*	0.4349
Surr08_ns	0.5026	*Surr08_es*	0.4238
Surr09_ns	0.4888	*Surr09_es*	0.4366
Surr10_ns	0.4846	*Surr10_es*	0.4274
Surr11_ns	0.4874	*Surr11_es*	0.4261

Surr12_ns	0.4948	*Surr12_es*	0.4266
Surr13_ns	0.4848	*Surr13_es*	0.4315
Surr14_ns	0.4824	*Surr14_es*	0.4245
Surr15_ns	0.4690	*Surr15_es*	0.4279
Surr16_ns	0.4882	*Surr16_es*	0.4253
Surr17_ns	0.4780	*Surr17_es*	0.4292
Surr18_ns	0.4795	*Surr18_es*	0.4299
Surr19_ns	0.4798	*Surr19_es*	0.4270

4.1.3. Power Spectral Density

The Fourier transform of a function *s(t)* is given by:

$$\tilde{s}(f) = \frac{1}{\sqrt{2\pi}} \int_{-\infty}^{+\infty} s(t) e^{2\pi i f t} dt \tag{15}$$

and that of a finite, discrete time series by

$$\tilde{s}_k = \frac{1}{\sqrt{N}} \sum_{j=1}^{N} s_j e^{2\pi i k n / N} \tag{16}$$

Here, the frequencies in physical units are $f_k = k/(N\Delta t)$, where $k = -N/2, \ldots, N/2$ and Δt is the sampling interval (1 hour in our case). The power spectrum of a process is defined to be the squared modulus of the continuous Fourier transform, $P(f) = |\tilde{s}(f)|^2$. The power spectrum is particularly useful for studying the main frequencies in a system, since there will be sharper or broader peaks at the dominant frequencies and their integer multiples, the harmonics.

In Figures 7-8 we observe the power spectral density of Nord Pool time series. For both of them, we have found behaviour of the type

$$P(f) \propto \frac{1}{f^{\alpha}} \tag{17}$$

where α is a positive real number. The values of α for Nord Pool time series and their surrogates are listed in Tables 6-7.

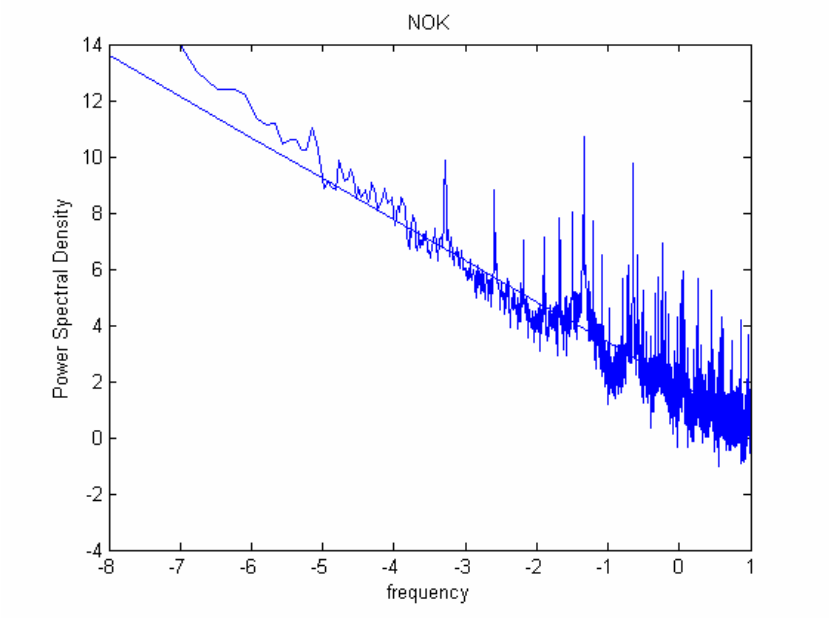

Figure 7. The power spectrum (log-log scale) , NOK (α=1.4612).

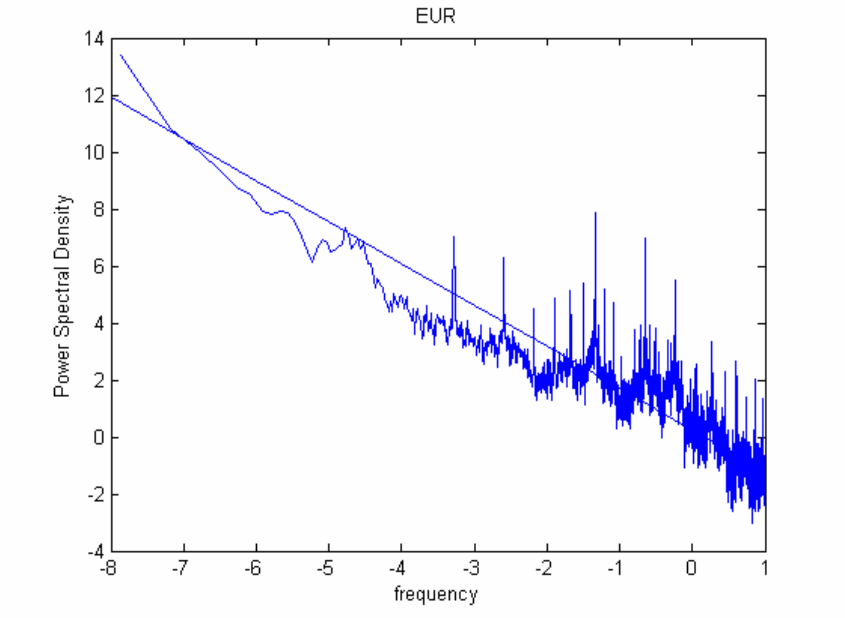

Figure 8. The power spectrum (log-log scale) EUR (□=1.4562).

Table 6. Power spectra trend α calculated using linear regression (LR) and Hurst exponent H. Real and linearly correlated data

Data set	α (LR)	α=2H+1	Data set	α(PS)	α=2H+1
NOK	1.4612	1.8812	*EUR*	1.4562	1.5346
Surr01_nl	1.3626	1.7264	*Surr01_el*	1.4281	1.2462
Surr02_nl	1.3577	1.7648	*Surr02_el*	1.4453	1.1798
Surr03_nl	1.3527	1.6798	*Surr03_el*	1.4296	1.2804
Surr04_nl	1.3440	1.7292	*Surr04_el*	1.4546	1.3262
Surr05_nl	1.4719	1.6552	*Surr05_el*	1.3914	1.3194
Surr06_nl	1.4085	1.8302	*Surr06_el*	1.4300	1.2650
Surr07_nl	1.3383	1.6960	*Surr07_el*	1.4140	1.1828
Surr08_nl	1.3628	1.6994	*Surr08_el*	1.4131	1.4524
Surr09_nl	1.3406	1.6250	*Surr09_el*	1.4558	1.2126
Surr10_nl	1.3566	1.6048	*Surr10_el*	1.4289	1.3346
Surr11_nl	1.3564	1.6792	*Surr11_el*	1.4466	1.2868
Surr12_nl	1.3301	1.7248	*Surr12_el*	1.4404	1.3224
Surr13_nl	1.3652	1.7590	*Surr13_el*	1.4276	1.3980
Surr14_nl	1.3767	1.7204	*Surr14_el*	1.4330	1.3208
Surr15_nl	1.3690	1.7148	*Surr15_el*	1.4341	1.2736
Surr16_nl	1.3701	1.6812	*Surr16_el*	1.4506	1.4192
Surr17_nl	1.3589	1.7748	*Surr17_el*	1.4455	1.3628
Surr18_nl	1.3483	1.6738	*Surr18_el*	1.4554	1.2178
Surr19_nl	1.3646	1.7548	*Surr19_el*	1.4666	1.1810

Table 7. Power spectra trend α calculated using linear regression (LR) and Hurst exponent H. Real and shuffled data

Data set	α (LR)	α=2H+1	Data set	α(PS)	α=2H+1
NOK	1.4612	1.8812	*EUR*	1.4562	1.5346
Surr01_ns	0.0100	1.0200	*Surr001_es*	0.0139	1.0278
Surr02_ns	0.0106	1.0212	*Surr002_es*	0.0148	1.0296
Surr03_ns	0.0150	1.0300	*Surr003_es*	0.0084	1.0168
Surr04_ns	0.0294	1.0588	*Surr004_es*	0.0237	1.0474
Surr05_ns	0.0200	1.0400	*Surr005_es*	0.0097	1.0194
Surr06_ns	0.0151	1.0302	*Surr006_es*	0.0019	1.0038
Surr07_ns	0.0212	1.0424	*Surr007_es*	0.0153	1.0306
Surr08_ns	0.0099	1.0198	*Surr008_es*	0.0126	1.0252
Surr09_ns	0.0243	1.0486	*Surr009_es*	0.0147	1.0294
Surr10_ns	0.0208	1.0416	*Surr010_es*	0.0138	1.0276
Surr11_ns	0.0216	1.0432	*Surr011_es*	0.0208	1.0416
Surr12_ns	0.0183	1.0366	*Surr012_es*	0.0137	1.0274
Surr13_ns	0.0218	1.0436	*Surr013_es*	0.0114	1.0228
Surr14_ns	0.0265	1.0530	*Surr014_es*	0.0154	1.0308
Surr15_ns	0.0261	1.0522	*Surr015_es*	0.0182	1.0364
Surr16_ns	0.0124	1.0248	*Surr016_es*	0.0247	1.0494
Surr17_ns	0.0192	1.0384	*Surr017_es*	0.0177	1.0354
Surr18_ns	0.0160	1.0320	*Surr018_es*	0.0106	1.0212
Surr19_ns	0.0133	1.0266	*Surr019_es*	0.0201	1.0402

It has been observed experimentally (Shuster, 1995) that the power spectra of a large variety of physical systems diverge at low frequencies with a power low $1/f^{\alpha}$ (0.8<α<1.4).

The appearance of a scaling behaviour in the power spectrum of economic time series support further, according to Theiler (1991), the existence of a self-organisation with many degree of freedom for these series.

If the motion is a fractional Brownian motion (fBm) a relationship exists between the Hurst exponent and the scaling factor of the power low α , see Eq. (11). We have calculated α from Hurst and directly from the spectrum. The results are presented in Tables 6 and 7. In all the time series considered, real and surrogate, the values are significantly different. However, this is not conclusive since there is a certain amount of variability calculating the Hurst exponents as well as α that may be responsible for these differences in particular for the linear surrogate time series.

4.1.4. Fitting Nord Pool data with stable distributions

Stable distributions are a class of distributions that have the property of stability: if a number of independent and identically distributed (iid) random variables have a stable distribution, then a linear combination of these variables will have the same distribution, except for possibly different shift and scale parameters. Special cases of stable distributions include Gaussian, Cauchy and Levy distributions. They are described by four parameters the first two are $\alpha \in (0,2]$, an index of stability and $\beta \in [-1,1]$, a skewness parameter. α and β determine the shape of the distribution. The last parameters are $\gamma \in [0,\infty)$ a scale parameter and $\delta \in (-\infty,\infty)$ a location parameter.

A stable probability distribution is defined by the Fourier transform of its characteristic function $\varphi(t)$:

$$f(x;\alpha,\beta,\gamma,\delta) = \frac{1}{2\pi}\int_{-\infty}^{\infty}\varphi(t)e^{-itx}dt \tag{18}$$

where $\varphi(t)$ is given by

$$\varphi(t) = \exp\left[it\delta - |\gamma t|^{\alpha}\left(1 - i\beta\,\mathrm{sgn}(t)\Phi\right)\right] \tag{19}$$

and sgn(t) is just the sign of t and Φ is given by

$$\Phi = \tan(\pi\alpha/2) \tag{20}$$

for all α except α=1 in which case:

$$\Phi = -(2/\pi)\log(t) \tag{21}$$

There is no general analytic expression for a stable distribution. There are, however four special cases which can be analytically expressed:

a/ for α=2 the distribution becomes a Gaussian distribution with variance $\sigma^2 = 2\gamma^2$ and mean δ

b/ for α=1 and β=0 the distribution reduces to a Cauchy distribution with scale parameter γ and shift parameter δ

c/ for α=1/2 and β=1 the distribution reduces to a Levy distribution with scale parameter γ and shift parameter δ

d/ In the limit as $\gamma \rightarrow 0$ or as $\alpha \rightarrow 0$ the distribution will approach a Dirac delta function $\boldsymbol{\delta}(x-\delta)$

The heavy tail behaviour causes the variance of stable distribution to be infinite for $\alpha<2$ (if $\alpha=2$ the distribution is Gaussian).

Stable distributions have been proposed as a model for many types of physical and economic systems because many large data sets exhibit heavy tails and skewness. Anyway, while non-Gaussian stable distributions are heavy tailed, most heavy-tailed distributions are not stable.

In order to analyse these series we have fitted the histogram to the first difference, of each series with a stable distribution (Nolan, 1999), X~S(α,β,γ,δ;A), using the program STABLE for univariate data (http://www.cas.american.edu/~jpnolan). The last parameter A can be 0 or 1 respectively if the characteristic function is continuous in all four parameters or not. We will consider the first case A=0. A typical situation in these time series is the existence of a high number of zero values normally in correspondence with weekends or holidays. To compare the results, we have eliminated from the original series the points where the exchange rate was unchanged, i.e. the zero value. Table 8 summarizes the fitted parameters using the maximum likelihood estimation (Nolan, 1997 and 1999); whereas in figs. 9-10 the fit obtained using both approaches is shown. The other methods implemented in STABLE, i.e. quantile/fractile method and sample characteristic function, gave similar results.

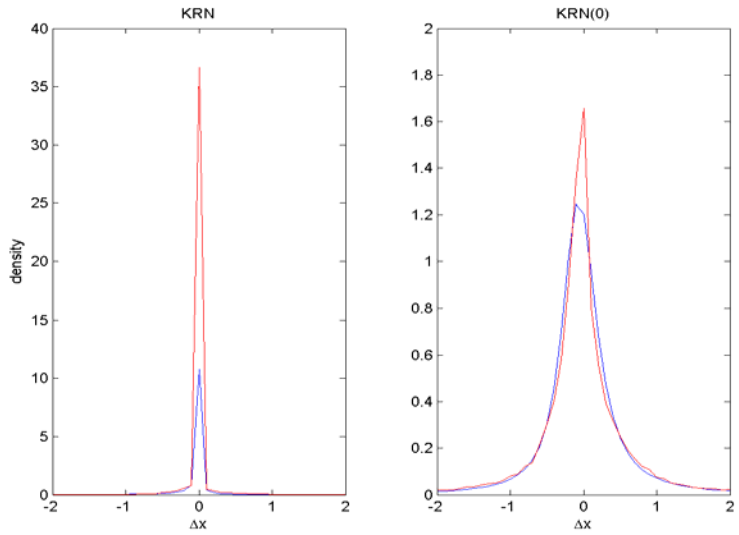

Figure 9. Fitted density plot for the Nord Pool Norwegian Krone time series data (blue line): a/Original time series, first difference; b/ without zero values (23962 values).

As can be observed in figs. 9 and 10, the first Nord Pool time series had a considerable amount of first differences equal to zero, i.e. no change between one spot price and the successive. This high value makes it difficult to fit a stable probability distribution (see fig. 9a). On the contrary, in the EUR Nord Pool time series this problem is not so evident and the stable parameters are quite similar with or without the zero values (see Table 8 and Fig. 10).

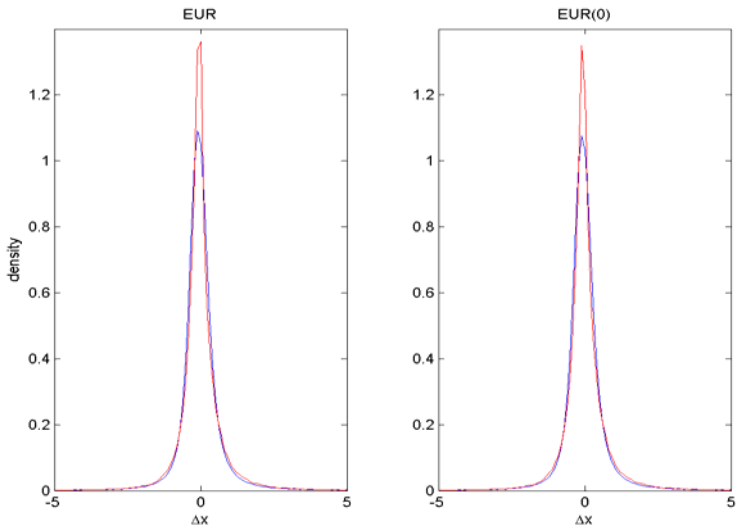

Figure 10. Fitted density plot for the Nord Pool Norwegian Euro time series data (blue line): a/Original time series, first difference; b/ without zero values (730 values).

Table 8. Nord Pool data fitted parameters using STABLE (Nolan, 1999).

Data set	α	β	γ	δ
KRN	0.412	-0.365	0.035	-0.00018
KRN(0)	1.116	0.127	0.242	-0.0514
EUR	1.308	0.164	0.268	-0.068
EUR(0)	1.315	0.173	0.272	-0.069

Afterwards, the surrogate time series for the Nord Pool in EUR have been compared with the original time series. The results are summarized in Table 9. The shuffled surrogate time series have all the same stable parameters as the original time series.

Table 9. Parameters of stable distribution that fit Nor Pool data in EUR/kwh and its surrogates linearly correlated.

Data set	α	β	γ	δ
EUR	1.308	0.164	0.268	-0.068
Surr01_nl	1.799	0.0397	1.16264	-0.6388E-2
Surr02_nl	1.7831	0.0264	1.13151	-0.61447E-2
Surr03_nl	1.6640	0.0378	1.02906	-0.0210
Surr04_nl	1.7762	0.0036	1.01902	0.1162E-2
Surr05_nl	1.8062	0.0205	1.11834	-0.3311e-2
Surr06_nl	1.6059	0.0011	0.903214	-0.66719E-2
Surr07_nl	1.7837	-0.0093	1.16422	0.30468E-2
Surr08_nl	1.7693	-0.0553	0.998577	0.15710E-1
Surr09_nl	1.7481	0.0135	1.18132	-0.22515E-2
Surr10_nl	1.7621	-0.0061	1.09915	0.35807E-2
Surr11_nl	1.7604	0.0624	1.13694	-0.27875E-1
Surr12_nl	1.7505	0.0450	1.07224	-0.15495E-1
Surr13_nl	1.7156	0.0161	1.05419	-0.827819E-2

Surr14_nl	1.7392	-0.0293	1.18483	0.67472E-2
Surr15_nl	1.7039	0.0619	1.00392	-0.15986E-1
Surr16_nl	1.7894	0.0155	1.10006	-0.69631E-2
Surr17_nl	1.8059	-0.0368	1.17309	0.87207E-2
Surr18_nl	1.7869	-0.0213	1.11810	0.60565E-2
Surr19_nl	1.7777	0.0038	1.19410	0.75471E-2

By comparing the surrogate data sets it is possible to observe that they have a probability distribution function (pdf) more similar to a Gaussian (α close to 2) in comparison with original data (α =1.308) and they have β closer to 0 which mean their pdfs have less skewness.

4.2. Finding the time delay and embedding dimension

Determining the time delay and the embedding dimension is considered as one of the most important steps in nonlinear time series modelling and prediction. A number of methods have been developed in determining the time delay and the minimum embedding dimension since the early beginning of nonlinear time series study. Here we will describe and apply several of them to the foreign exchange time series data sets.

4.2.1. Time delay

The first step in phase space reconstruction is to choose an optimum delay parameter □. Different prescriptions have appeared in the literature to choose □ but they are all empirical in nature and do not necessarily provide appropriate estimates:

- *First passes through zero of the autocorrelation function*: In earlier works (Mees *et al*., 1987) it was suggested to use the value of τ for which the autocorrelation function

$$C(\tau) = \sum_n [s(n) - \bar{s}][s(n+\tau) - \bar{s}] \tag{22}$$

first passes through zero which is equivalent to requiring linear independence.

The application of the zero crossing of the autocorrelation function gives quite high values for both time series, see Fig. 11.

- *First minimum of the Average mutual information*: Fraser and Swinney (1986) suggested to use the average mutual information (AMI) function, $I(\tau)$, as a kind of nonlinear correlation function to determine when the values of $s(n)$ and $s(n+\tau)$ are independent enough of each other to be useful as coordinates in a time delay vector but not so independent as to have no connection which each other at all. For a discrete time series, $I(\tau)$ can be calculated as,

$$I(\tau) = \sum_{n,n+T} P(s(n), s(n+\tau)) \log_2 \left[\frac{P(s(n), s(n+\tau)}{P(s(n))P(s(n+\tau))} \right] \tag{23}$$

where $P(s(n))$ refers to individual probability and $P(s(n),s(n+\tau))$ is the joint probability density. Following the method developed by Abarbanel (1996), to determine $P(s(n))$ we simply project the values taken form $s(n)$ versus n back onto the $s(n)$ axis and form an histogram of the values. Once normalised, this gives us $P(s(n))$. For the join distribution of $s(n)$ and $s(n+\tau)$ we form the two-dimensional histogram in the same way.

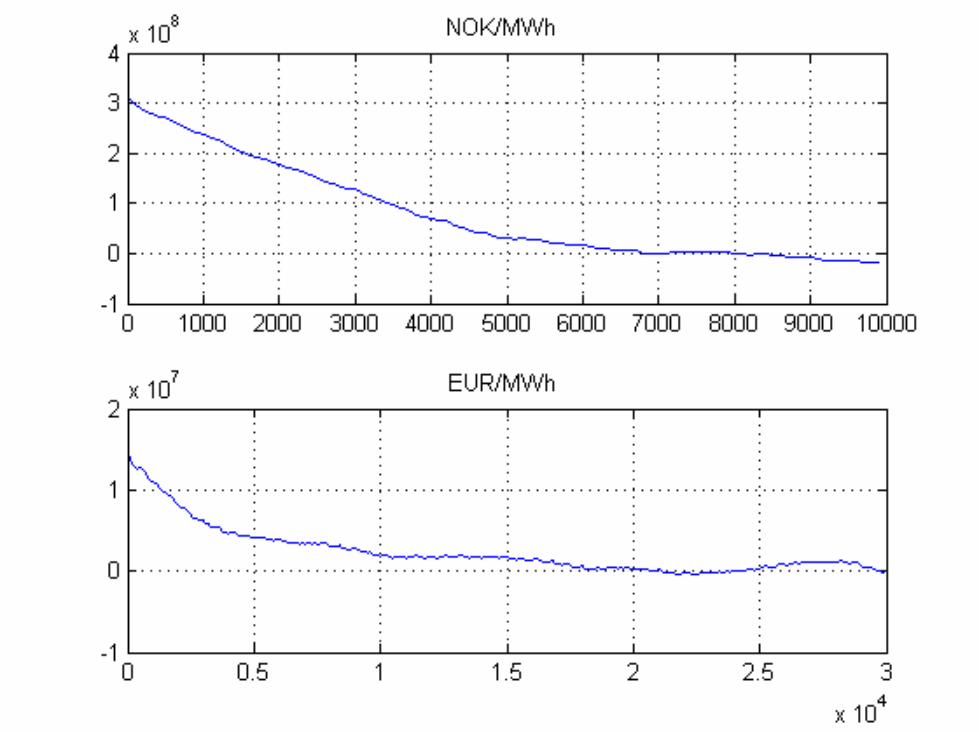

Figure 11. Correlation f of the Nord Pool time series.

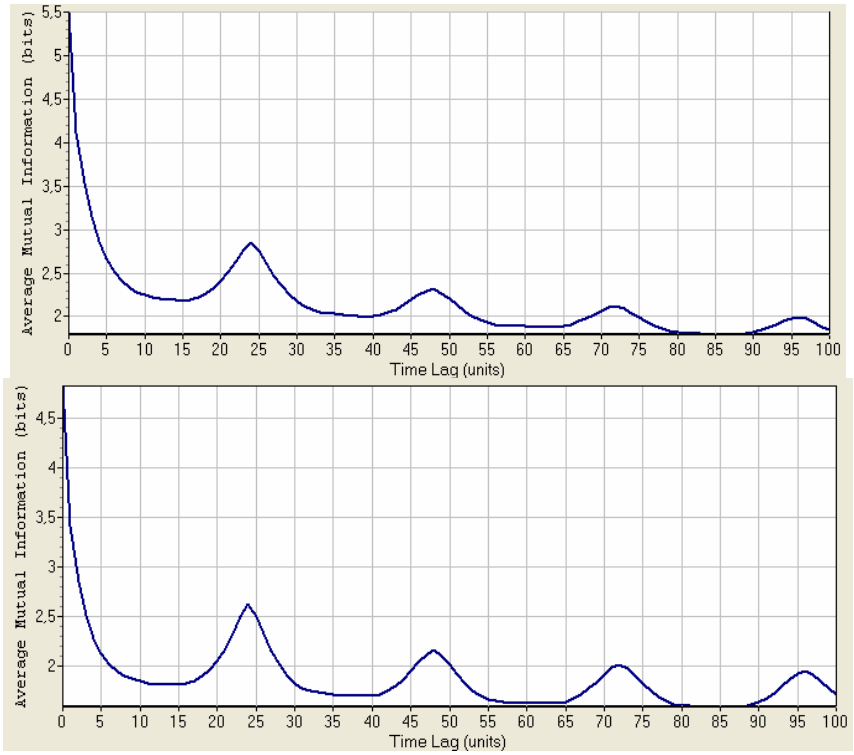

Figure 12. Average Mutual information function. First minimum for NOK/MWh time series (top) occurs at τ=15, whereas for the EUR/MWh time series (bottom) for τ=13.

In general, the time lag provided by $I(\tau)$ is normally lower than the one calculated with the $C(\tau)$, $\tau_{AMI} \geq \tau_{correl}$, and provides the appropriate characteristic time scales for the motion. Even though $C(\tau)$ is the optimum linear choice from the point of view of predictability in a least square sense of $s(n+\tau)$ from knowledge of $s(n)$, it is not clear why it should work for nonlinear systems and it has been shown that in some cases it does not work at all.

4.2.2. Embedding dimension

The dimension, where a time delay reconstruction of the system phase space provides a necessary number of coordinates to unfold the dynamics from overlaps on itself caused by projection, is called the embedding dimension, d_E. This is a global dimension, which can be different from the real dimension. Furthermore, this dimension depends on the time series measurement, and hence, if we measure two different variables of the system, there is no guarantee that the d_E from time delay reconstruction will be the same from each of them.

The usual method for choosing the minimum embedding dimension is to compute some invariant of the attractor. By increasing the embedding dimension used for the computations, one notes when the value of the invariant stops changing. Since these invariants are geometric properties of the dynamics, they become independent of d for $d \geq d_E$, i.e. after the geometry is unfolded.

In this work, we have used three methods:

- <u>*Saturation of the correlation dimension*</u>: The correlation dimension is a measure of the dimension obtained considering correlations between points. If N is the number of points in the time serie, τ is a fixed increment of time and $\{x_i\}_{i=1}^{T} \equiv \{x(t+i\tau)\}_{i=1}^{T}$ the *correlation integral* is defined as:

$$C(\varepsilon) = \lim_{T\to\infty} \frac{1}{T^2} \sum_{\substack{i,j=1 \\ i\neq j}}^{T} \Theta\left(\varepsilon - \left\| x_i - x_j \right\|\right) \tag{24}$$

where

$$\Theta(x) = \begin{cases} 1 & for\ x \geq 0 \\ 0 & otherwise \end{cases} \tag{25}$$

is the Heaviside function and ||.|| denote the Euclidean norm. The function $C(\varepsilon)$ behaves as a power of ε for small ε:

$$C(\varepsilon) \propto \varepsilon^{\nu} \tag{26}$$

the exponent ν is called *correlation dimension*.

The correlation dimension is frequently used to distinguish between chaotic and random behaviour. The idea behind it is to construct a function $C(\varepsilon)$ that is the probability that two arbitrary points on the orbit are closer together than ε. The correlation dimension is given by log(C)/log(ε) in the limit $\varepsilon \to 0$, and $N \to \infty$. The correlation dimension is defined as the slope of the curve C(ε) versus ε. C(ε) is the correlation of the data set, or the probability that any two points in the set are separated by a distance ε. A noninteger result for the correlation dimension indicates that the data is probably fractal. In VRA, $C(\varepsilon)$ is calculated for every embedding dimension specified in the range and plotted against that range. For the truly random signals, the

correlation dimension graph will look like a 45-degree straight line, indicating that no matter how you embed the noise, it will evenly fill that space. Chaotic (and periodic) signals, on the other hand, have a distinct spatial structure, and their correlation dimension will saturate as some point, as embedding dimension is increased.

For our two time series the saturation does not occur at least until of an embedding dimension of 20, but this can be due to the presence of noise in the signal.

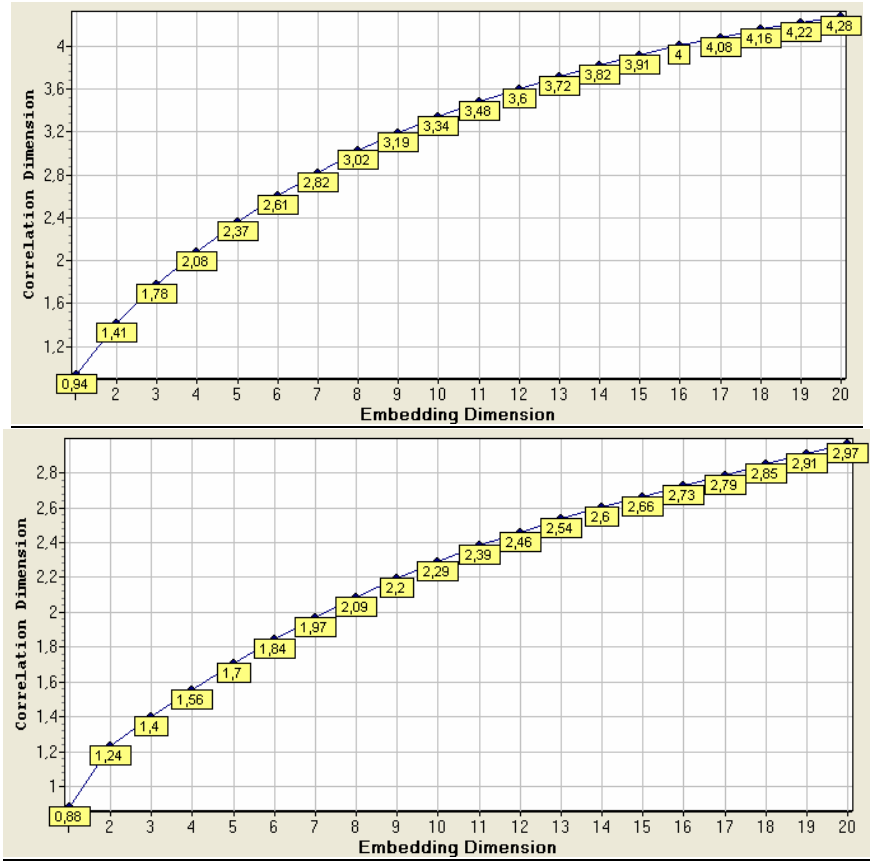

Figure 13. Correlation dimension for NOK/MWh time series (top), and EUR time series (bottom).

- *False Nearest Neighbours*: The method of False Nearest Neighbours (FNN) was developed by Kennel *et. al* (1992). In this case, the condition of no self-intersection states that if the dynamics is to be reconstructed successfully in R^d, then all the neighbour points in R^d should be also neighbours in R^{d+1}. The method checks the neighbours in successively higher embedding dimensions until it finds only a negligible number of false neighbours when increasing dimension from d to $d+1$. This d is chosen as the embedding dimension.

It was found by Kennel *et al.* (1992) that if the data set is clean from noise, the percentage of false nearest neighbours will drop from nearly 100% in dimension one to strictly zero when d_E is reached. Further, it will remain zero from then on since the dynamics is unfolded. If the signal is contaminated with noise (infinite dimension signal) we may not see the percentage of false nearest neighbours drop to near zero in any dimension. In this case, depending on the signal to noise ratio the determination of d_E will degrade.

For both time series, the FNN method suggest an embedding dimension of 6, see fig 14. The increase of the number of FNN after a certain d_E is an indication of the presence of noise in the signal.

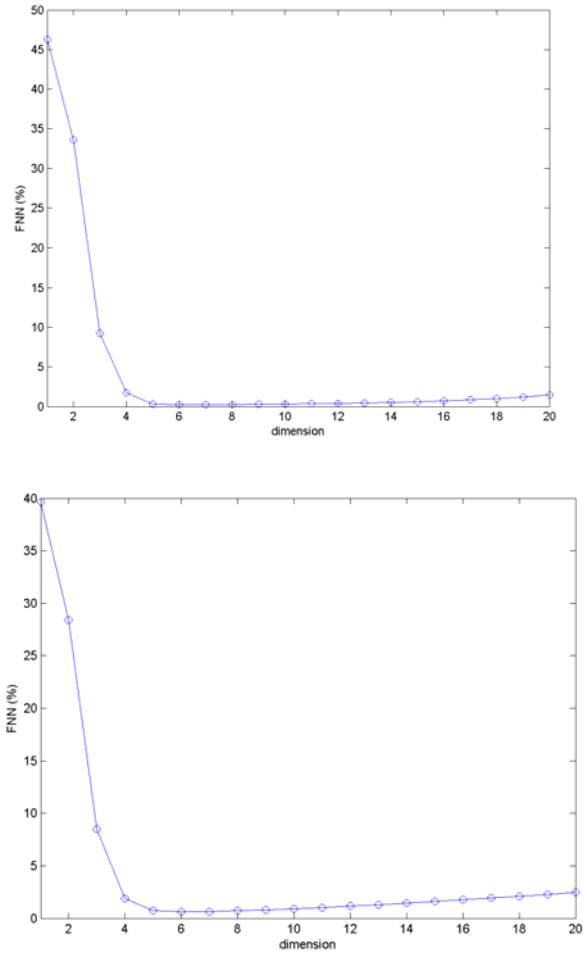

Figure 14. Embedding dimension using the FNN method. a/NOK/MWh time series; b/ EUR/MWh time series.

- *E1 & E2 Method* : The method of FNN has some subjectivity in defining that a neighbour is false since the values of two threshold parameters have to be defined, Kennel *et. al* (1992). To improve this situation, Cao (1997) developed a similar method, which is based on evaluating the mean value of the distance between time-delay vectors, *E1(d)*. However, if we look only to the quantity *E1(d)* we can obtain wrong results in the case of random signals. For time series data from a random set of numbers *E1(d)*, in principle, will never reach a saturation value as *d* increase. But in practical computations, it is difficult to resolve whether the *E1(d)* is slowly increasing or has stopped changing if d is sufficiently large. In Fact, since available observed data samples are limited, it may happen that the *E1(d)* stop changing at some *d* although the time series is random. To solve this problem Cao (1997) suggested to consider the quantity *E2(d)*. Let $y_i(d) = \{s(i), s(i+\tau), ..., s(i+(d-1)\tau\}$ and $y_{n(i,d)}$ the nearest neighbour of $y_i(d)$ in the d-dimensional reconstructed state space, then it is possible to define:

$$E^*(d) = \frac{1}{N - d\tau} \sum_{i=1}^{N-d\tau} \left| s_{i+d\tau} - s_{n(i,d)+d\tau} \right| \qquad (27)$$

$$E2(d) = \frac{E*(d+1)}{E*(d)} \tag{28}$$

Since the future values are independent of the past values, *E2(d)*, for random data, will be equal to 1 for any *d*. However, for deterministic data, *E2(d)* is certainly related to *d*, and it cannot be a constant for all *d*. In other words, there must exist some *d*'s such that *E2(d)≠1*. The E1&E2 method depends only on the time delay, and the embedding dimension is calculated, as in the other methods, when the values of E1 and E2 reach saturation. Cao (1997) showed that the method does not strongly depend on how many points are available, provided there are enough and it can clearly distinguish between deterministic and stochastic.

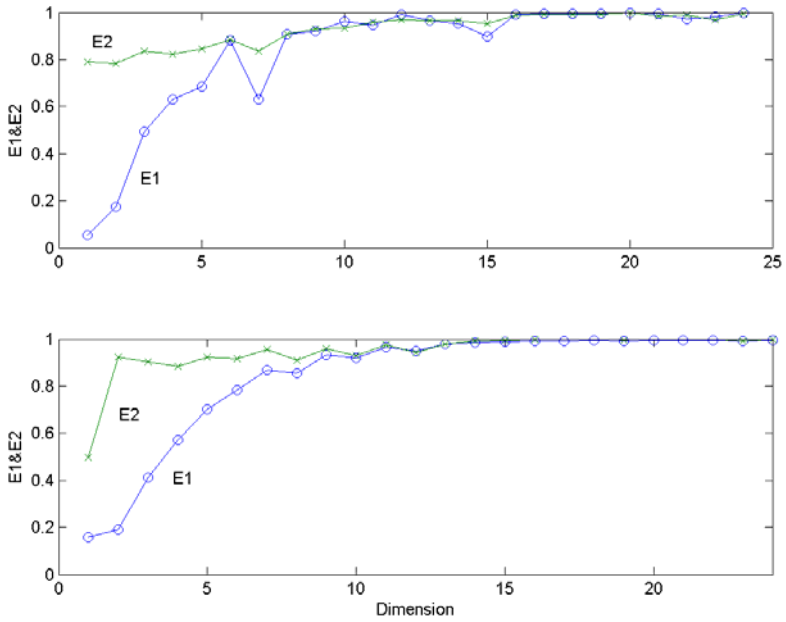

Figure 15. Embedding dimension calculation for the Nord pool time series. NOK/MWh (top), EUR/MWH (bottom).

Table 10 summarises the results obtained analysing Nord Pool time series. The time delay has been obtained using the first minimum of the AMI, Eq. (23). The embedding dimension has been computed using the methods of FNN (Kennel *et al.*, 1992) and the E1&E2 method (Cao, 1997). The results of this last method can be seen by looking at the value of *E2* (fig 15), furthermore it can be also observed that the time series analysed does not behave as stochastic signals, i.e. *E2*≈1 for all *d*. Furthermore, both time series have high dimensionality, $d_E \geq 7$. This high values are in agreement with similar analysis carried out by Cao (2002) for other economic time series, i.e. daily variations in the British Pound and Japanese Yen/US dollar.

Table 10. Time delay, τ, and embedding dimension, d_E, found for the Nord Pool data sets.

Data set	**τ**	**d_E (FNN)**	**d_E (E1&E2)**
NOK/MWh	15	7	10
EUR/MWh	13	6	10

4.3. Detecting non-stationarity

Broadly speaking a time series is said to be stationary if there is no systematic change in mean (no trend), in variance, and, if strictly periodic variations have been removed. Most of the probability theory of time series is concerned with stationary time series, and for this reason time series analysis often requires one to turn a non-stationary series into a stationary one so as to use this theory. However, it is also worth stressing that the nonstationary components, such as the trend, may sometimes be of more interest than the stationary residual.

We only report here a relatively simple stationarity test, called *space time separation plot (stp)*, introduced by Provenzale *et al*. (1992). The idea below is that in the presence of temporal correlations the probability that a given pair of state points in the reconstructed state space, $\{s(t_i), s(t_i-\Delta t), s(t_i-2\Delta t),\ldots\}$, has a distance smaller than *r*, i.e. $\|\mathbf{s}_i-\mathbf{s}_j\| < r$, does not depend only on the position of the sate but also on the time that has elapsed between them. This dependence can be detected by plotting the number of neighbour points as a function of two variables, the time separation and the spatial distance. In principle, one can create for each time separation an accumulated histogram of spatial distances. In the case of power-law noises the only points with small spatial separation are dynamically near neighbours, i.e. the series is non-recurrent in phase space. In this case the contour curves do not saturate. In the case of stationarity, we will find saturation in the plot.

Figures 16 show the results of the test to the analysed time series. In those graphics the separation time is represented in the horizontal axis whereas the base 2 logarithm of the separation in space is represented in the vertical axis. For small Δt points are always near neighbours in space, as their time separation increases so does their separation in space, in principle (Provenzale *et al*. 1992). Technically we have to create, for each time separation Δt an accumulate histogram of spatial distance ε. We have used the program *stp* of Tisean (Kantz and Schreiber, 1997) which returns level lines for 10%, 20%, … of the pairs with a given temporal separation Δt.

As can be observe the Nord Pool time series saturate, Fig. 16a, 16c but the high frequency exchange rates do not (Strozzi *et al*., 2002), fig. 16b and 16d, which gives the indication that Nord Pool time series are more stationary than other financial high frequency series. The non saturation, a part from the non-stationarity, is an indication that the data we are analysing has significant power in the low frequency, such as 1/f noise or Brownian motion. In this case, all points in the data set are temporally correlated and there is no way of determining an attractor dimension from the sample. A similar situation arises if the data set is too short. Then there are no pair left after removing temporally correlated pairs. If we regard the problem from a different point of view, correlation times of the order of the length of the sample (nonsaturating curves) mean that the data does not sample the observed phenomenon sufficiently (Kantz and Schreiber, 1997).

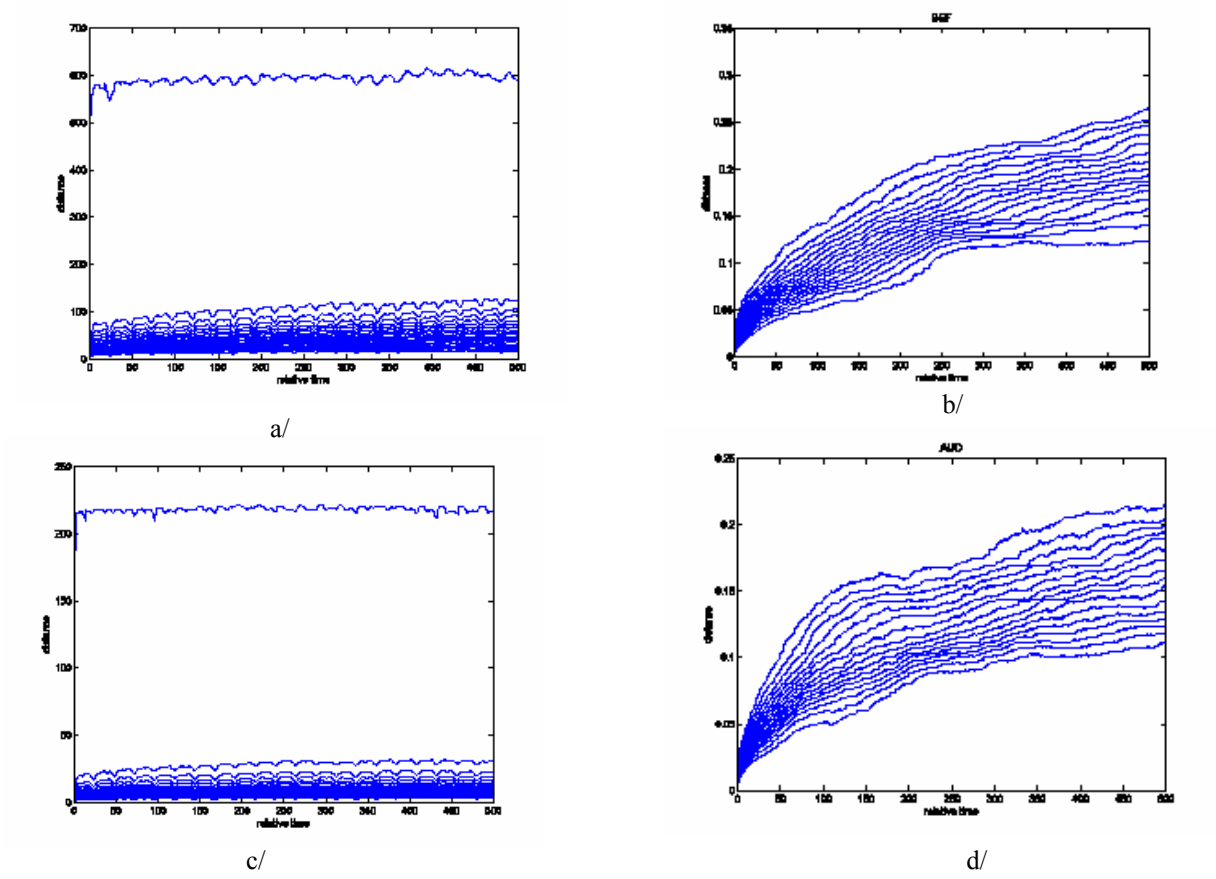

Figure 16. a/ Space-time separation plot (stp) of the Nord Pool spot prices (NOK/MWh); b/ Space-time separation plot of Australian-US dollar foreign exchange time series; c/ Space-time separation plot of the Nord Pool spot prices (EUR/MWh); d/ Space-time separation plot Belgium Franc-US dollar foreign exchange time series .

In Figure 17 we have plotted the space-time separation plot for several of the surrogates time series. As it is possible to observe, in the case of linear surrogates, the results are very similar to the ones obtained for the real time series. In addition, the space-time separation plots finds that the series are stationary.

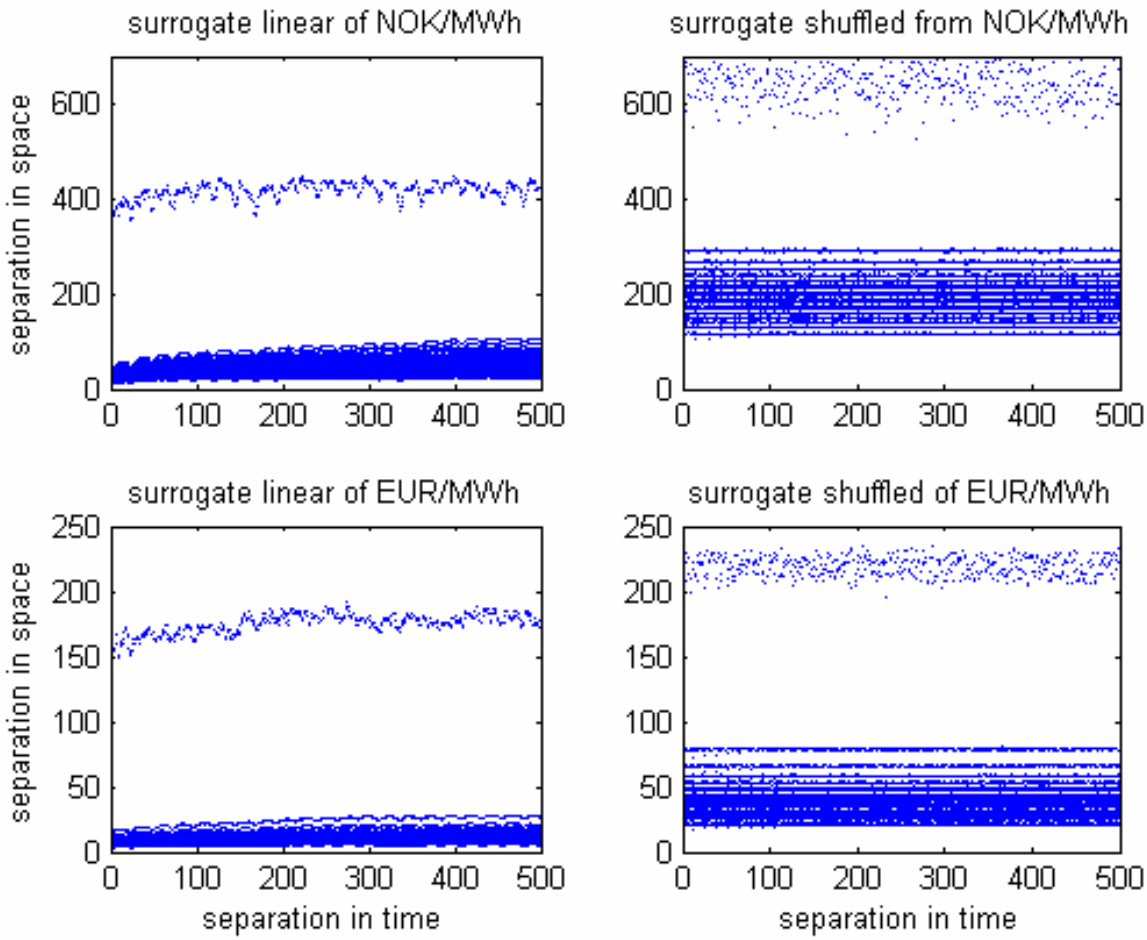

Figure 17. Space-time separation plot (stp) of the surrogate time series.

4.4. Testing for non-linearity

The former tests using surrogate data sets concerning the Hurst exponent, power spectrum and the stable distribution give an idea of the characteristics of the original series when compared with their surrogates. However, we have not tested the original time series for the existence of determinism. For this we need some parameter that is related with low dimensional determinism in the series. In order to test the null hypothesis that the series is a linear Gaussian random series with a 95% significance level, we have used the surrogate data sets for each Nord pool spot prices time series and as parameter, we have considered the error in the nonlinear one step ahead prediction (Farmer and Sidorowich, 1987). For both Nord Pool time series, the null hypothesis can be rejected since the prediction error is found to be smaller in the original time series that that of the surrogate data sets. These results are in agreement with the previous findings of the space time separation plot in which one can see that the curves saturate which means that the system is in principle not completely stochastic. However, we have also carried out another test based on time reversal symmetry statistic and in this case the null hypothesis, i.e. that a linear Gaussian random processes, cannot be rejected since the time asymmetry of the data was found to be not significantly different from that of the *surrogates*. These inconclusive results are typical of financial time series (Strozzi *et al*., 2002).

4.5. Recurrence quantification analysis (RQA)

The actual methods developed in non-linear time series analysis assume that the data series under analysis have reach their attractors and that there are not in a transient phase, that they are autonomous and that their lengths are much longer than the characteristic time of the system in question. In the case of Nord Pool spot prices time series these assumptions are not clearly confirmed by the preliminary analysis and it may be useful to have another procedure to analyse these data**.**

Eckmann *et al*. (1987) introduced a new graphical tool, which they called a recurrence plot (RP). The recurrence plot is based on the computation of the distance matrix between the reconstructed points in the phase space, i.e. $\mathbf{s}_i=\{s(t), s(t-\tau), s(t-2\tau),...s(t+(d_E-1)\tau\}$,

$$d_{ij} = \left\| \mathbf{s}_i - \mathbf{s}_j \right\| \tag{29}$$

This produces an array of distances in a NxN square matrix, **D**, being N the number of points under study. Once this distance matrix is calculated, in the original paper of Eckmann *et al*. (1987), it was displayed by darkening the pixel located at specific (i,j) coordinates which corresponds to a distance value between i and j lower than a predetermined cutoff, i.e. a ball of radius ε centered at $\mathbf{s}_i$. Requiring $\varepsilon_i = \varepsilon_j$, the plot is symmetric and with a darkened main diagonal correspondent to the identity line. The darkened points individuate the recurrences of the dynamical systems and the recurrent plot provides insight into periodic structures and clustering properties that are not apparent in the original time series.

4.5.1. *Selection of the threshold or cutoff value ε*

A crucial parameter of a recurrence plot is the threshold ε. If ε is chosen too small, there may be almost no recurrence points and we will not be able to learn about the recurrence structure of the underlying system. On the other hand, if ε is chosen too large, almost every point is a neighbour of every other point. A too large ε includes also points into the neighbourhood which are simple consecutive points on the trajectory. Hence, we have to find a compromise for the ε value. Moreover, the influence of noise can bring us to choose a larger threshold, because noise would distort any existing structure in the RP. At higher threshold, this structure may be preserved. Several "rules of thumb" for the choice of the threshold ε are present in the literature between them (Marwan *et al*., 2007):

a/ it should not exceed 10% of the mean or the maximum phase space diameter (Koebbe and Mayer-Kress, 1992; Zbilut and Webber, 1992)

b/ it should be such that the recurrence point density in RP is approximately 1% (Zbilut *et al.*, 2002)

c/ in order to avoid problem related to noise, ε has to be chosen such that it is five time larger than the standard deviation of the observational noise, i.e. $\varepsilon>5\sigma$ (Thiel *et al*., 2002)

Nevertheless, the choice of e depends strongly on the considered system under study.

In Fig. 20 we have plotted the RP for both Nord Pool time series. We choose the 10% of the maximum phase space diameter as cutoff value. Several regime shifts are evident in both time series. A regime shift can be identified by squares structures of points separated by empty spaces (Zaldívar *et al*. 2007). However, in spite

of the differences, it is not evident how to connect the RPs with important facts in the dynamic of the underlying process. For doing this we need recurrence quantification parameters provided by RQA.

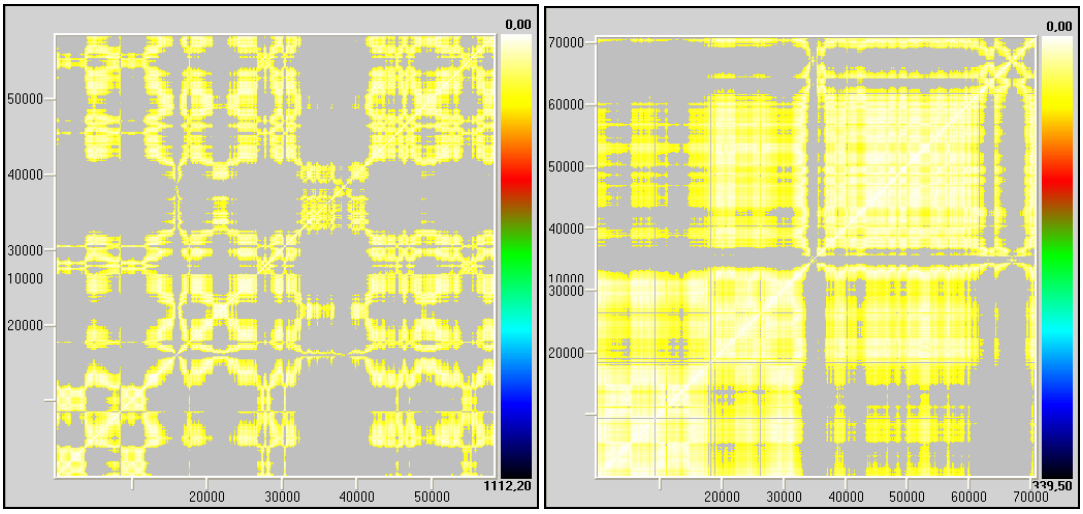

Figure 20 a). RP for NOK/MWh τ=15, d_E=10, ε=40 (left) and for EUR/KMh τ =13, d_E =10, ε=10 (right)

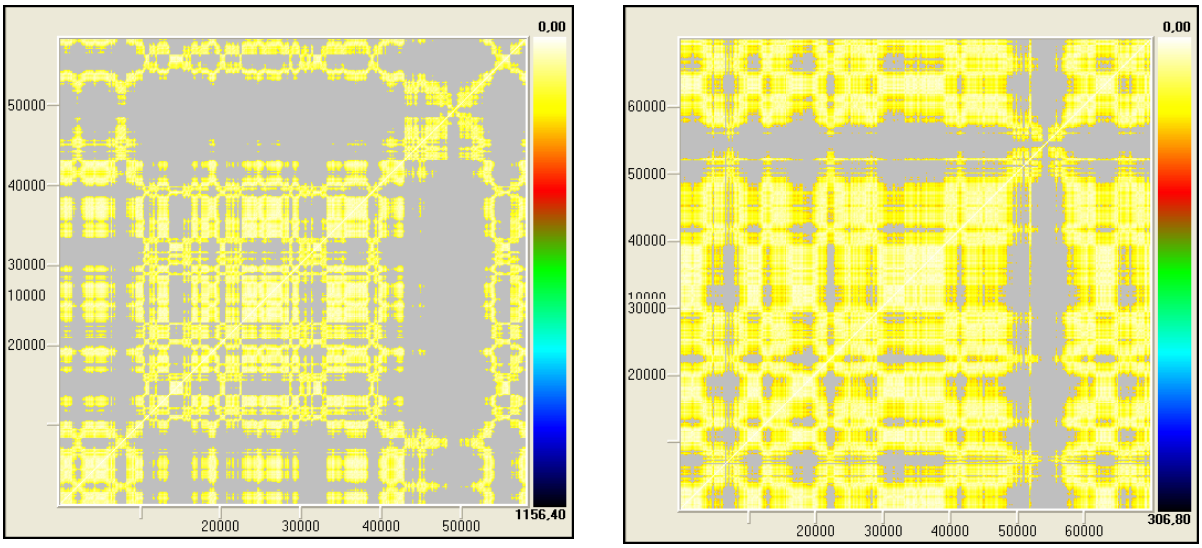

a/ b/

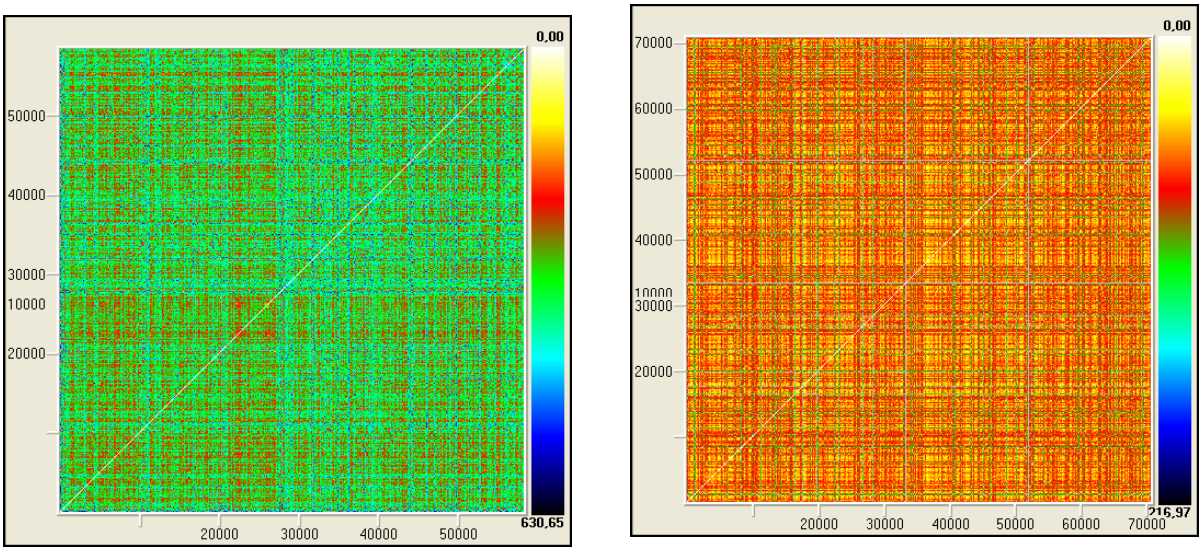

c/ d/

Figure 21. RPs of linear Gaussian surrogates: a/ NOK/MWh τ=15, d_E=10, ε=40; b/ EUR/KMh τ =13, d_E =10, ε=10. RPs of shuffled surrogates: c/ NOK/MWh τ=15, d_E=10, ε=40; d/ EUR/KMh τ =13, d_E =10, ε=10.

In fig 21 we have plotted the RPs for Gaussian linearly correlated and shuffled surrogate time series, respectively. Looking to fig. 20a and 20b, it can be observed that RPs of linear surrogate are qualitatively similar in the structure as those of the real time series, whereas RPs of shuffled data have no particular structures, see fig. 21c and 21d. RPs are then a tool for detecting correlations in the dynamics, but the question on how quantifying these RPs arises. This is necessary in order to distinguish, for example figures such as 20 and 21.

4.5.2. Quantification of the Recurrence Plots

Zbilut and Webber (1992) developed a methodology called Recurrence Quantification Analysis (RQA) with the aim of quantifiying RP´s structures. As a result, they defined several measures of complexity to quantify the small scale structures in RP. These measures are based on the recurrence point density and the diagonal and vertical line structures of the RP. A computation of these measures in small windows (sub-matrices) of the RP moving along the main diagonal yields the time dependent behaviour of these variables (Weber and Zbilut, 1994). Some studies based on RQA measures show that they are able to identify bifurcation points, especially chaos-order transitions (Trulla *et al*., 1996). The vertical structures in the RP are related to intermittency and laminar states: those measures quantifying the vertical structures enable to detect chaos-chaos transitions (Marwan *et al*., 2002). The measures to quantify complexity of RPs are the following:

a/ Measures based on recurrence density

%recurrence (RR) is the percentage of darkened pixels in recurrence plot:

$$RR(\varepsilon) = \frac{1}{N^2}\sum_{i,j=1}^{N}\mathbf{R}_{i,j}(\varepsilon) \qquad (30)$$

where $\mathbf{R}_{i,j}(\varepsilon)$ is one if the state of the system at time I and the one at time j have a distance less than ε and zero otherwise.

It is a measure of the density of recurrence points in RP. Note that it corresponds to the definition of the correlation integral, Eq. (24), except that the points of the main diagonal usually are not included.

b/ Measures based on diagonal lines

Let P(ε,l) be the histogram of diagonal lines of length l. If we assume we have obtained the right value of ε then we can consider $P(\varepsilon, l) = P(l)$. Processes with uncorrelated or weakly correlated behaviour cause none or very short diagonals, whereas deterministic processes cause longer diagonals. It is called *%determinism* (DET) the ratio of recurrence points that form diagonal structures (of at least length l_{min}) to all recurrence points

$$DET = \frac{\sum_{l=l_{\min}}^{N} lP(l)}{\sum_{l=1}^{N} lP(l)} \tag{31}$$

%determinism (DET) is then the percentage of recurrent points forming diagonal line structures. If l_{min} =1 the determinism is one. For the choice of l_{min} we have to take into account that the histogram P(l) can become sparse if l_{min} is too large, and, thus, the reliability of DET decreases.

Another RQA measure considers the length $L_{\max}$ of the longest diagonal line found in the RP, or its inverse, the divergence (DIV)

$$L_{\max} = \max\left(\{l_i\}_{i=1}^{N_l}\right), \text{ respectively } DIV = \frac{1}{L_{\max}} \tag{32}$$

where $N_l = \sum_{l \geq l_{\min}} P(l)$ is the total number of diagonal lines.

These measures are related to the exponential divergence of the phase space trajectory. The faster the trajectory segments diverge, the shorter are the diagonal lines and the higher is DIV.

The measure *entropy* (ENTR) refers to the Shannon entropy of the probability $p(l) = P(l)/N_l$ to find a diagonal line of length l in RP.

$$ENTR = -\sum_{l=l_{\min}}^{N} p(l) \ln p(l) \tag{33}$$

ENTR reflects the complexity of the RP in respect of the diagonal lines. For uncorrelated noise the value of ENTR is rather small, indicating its low complexity.

Trend is a measure of the paling recurrence points away from the central diagonal. It is a linear regression coefficient over recurrence point density of the diagonals parallel to main diagonal as a function of the time distance between these diagonals and the main diagonal. It provides information about non-stationarity in the process, especially if a drift is present in the trajectory. Trend will depend strongly on the size of the window and may yield ambiguous results for different window sizes.

c/ Measures based on vertical lines

We can find vertical lines in presence of laminar states in intermittence regimes. Let the total number of vertical lines of length ν in RP is given by the histogram $P(v)$ and, analogous to the definition of the determinism, the ratio between the recurrence points forming the vertical structures and the entire set of recurrence points can be computed:

$$LAM = \frac{\sum_{v=v_{\min}}^{N} vP(v)}{\sum_{v=1}^{N} vP(v)} \tag{34}$$

This it is called *laminarity*. The computation of LAM is realised for those ν that exceed a minimal length ν_{min}. LAM represents the occurrence of laminar stares in the system without describing the length of these laminar phases. LAM will decrease if the RP consists of more single recurrence points than vertical structures.

The average length of vertical structures is given by

$$TT = \frac{\sum_{v=v_{\min}}^{N} vP(v)}{\sum_{v=v_{\min}}^{N} P(v)} \tag{35}$$

and is called *Trapping Time*. *TT* estimates the mean time that the system will abide at a specific state or how long the state will be trapped.

In contrast to the RQA measures based on diagonal lines, these measures are able to find chaos-chaos transitions. Since periodic dynamics the measures quantifying vertical structures are zero, chaos-order transition can be identified (Marwan et al., 2002).

For a recent overview of the quantifying techniques and their applications, the reader is referred to Marwan et al. (2007).

4.5.3. Analysing the complete time series

In order to check if RQA measures are able to distinguish between real data and their surrogates (linear Gaussian processes) we calculated all of them for both. The results are summarized in Tables 11-12 for NOK/MWh and EUR/MWh time series, respectively.

Table 11. RQA measures for NOK/MWk original time series ant its surrogates linear correlated.

Data set	*%recur*	*%deter*	maxline	entropy	trend	% laminar	TrapTime
Bpr	16.095	67.13	3545	8.593	-8.687	69.994	308.044
Surr001	8.150	6.129	4808	6.740	2.306	1.796	123.511
Surr002	1.926	4.521	1355	4.913	-0.142	0.000	-1
Surr003	2.807	8.026	4808	6.028	-1.616	0.000	-1
Surr004	30.218	36.309	4808	7.994	-3.360	35.521	214.805
Surr005	1.735	13.216	1844	6.117	-0.983	0.055	110
Surr006	1.007	32.018	1178	6.287	-0.752	16.980	166.134
Surr007	4.785	13.279	2674	6.895	-0.802	7.533	153.511
Surr008	14.122	17.880	4350	7.357	-4.479	9.293	154.815
Surr009	5.934	13.528	3130	7.195	-2.458	6.301	159.498
Surr010	1.193	5.900	1064	4.696	-0.677	0.347	119.500
Surr011	4.860	51.638	4808	7.918	-1.542	52.444	266.162
Surr012	31.899	52.675	4808	8.415	12.407	54.522	218.168
Surr013	4.795	9.417	4808	6.880	0.524	0.724	143.393
Surr014	5.725	9.169	4154	6.783	-2.980	1.774	144.963
Surr015	4.972	6.340	2370	6.606	-2.341	1.720	114.988
Surr016	18.050	23.404	4808	7.678	-4.183	12.845	161.470
Surr017	10.846	43.188	4614	8.799	-7.222	38.298	338.899
Surr018	4.956	8.523	4808	6.596	-2.654	3.484	141.553
Surr019	6.323	4.462	4808	6.184	-1.989	0.375	114.208

Trapping Time = -1 means that no vertical lines were found.

Table 12. RQA measures for EUR/MWk time serie ant its surrogates linear corelated.

Data set	*%recur*	*%deter*	maxline	entropy	trend	% laminar	TrapTime
Beur	7.12	35.33	2094	7.658	-4.587	33.94	263.525
Surr001	12.524	3.665	3340	6.355	-6.259	2.539	149.367
Surr002	1.643	5.894	2238	5.270	-1.100	1.872	119.367
Surr003	3.840	1.397	2150	4.533	-0.998	0.000	-1
Surr004	4.377	1.105	1324	3.970	-0.286	0.000	-1.000
Surr005	10.677	1.825	4187	5.730	-5.483	1.527	126.613
Surr006	8.658	18.813	4826	7.538	-5.638	9.854	146.364
Surr007	0.491	3.888	690	2.807	-0.346	0.000	-1.000
Surr008	23.790	11.105	4826	7.509	-7.639	9.252	162.159
Surr009	30.269	10.831	4826	7.393	-1.830	7.108	151.053
Surr010	20.536	4.700	4826	6.845	-7.466	6.416	150.611
Surr011	2.336	3.777	1888	5.094	-1.160	1.529	134.161
Surr012	3.715	1.475	3517	4.059	-1.627	0.108	117.250
Surr013	4.994	3.736	3721	5.972	-3.343	1.886	135.457
Surr014	21.649	9.020	4826	7.162	-2.900	9.664	154.810
Surr015	20.052	8.142	2669	7.247	-4.243	4.171	146.484
Surr016	6.811	5.384	3998	6.574	-4.098	0.758	125.312
Surr017	3.161	4.113	1964	5.641	-2.076	0.715	131.650
Surr018	7.809	3.369	2429	6.204	-0.473	2.766	132.437
Surr019	12.185	1.330	4826	5.429	1.503	0.088	125.600

By looking to Tables 11-12 we can observe that *%recurrence*, *maxline*, *entropy*, *trend* or *Trapping Time* parameters cannot distinguish, with a 95% of confidence, between a linear gaussian dynamic and the dynamic behind the financial time series. Of course this does not implies that are not useful for their quantification, but only that the values of the parameters are in some case higher and in other cases smaller than those of the original time series. On the contrary, using *%determinism*, *%laminarity* we obtain values which are always smaller for surrogate data in comparison with original data sets. The fact that these two parameters are able to distinguish between the original time series and the surrogate time series points toward the explanation that the original series have more diagonal and vertical lines, and therefore their state remain near or at the same place longer in time more often than for their surrogate linear Gaussian process and that they posses a different decaying of the autocorrelation function. It could be interesting to generate surrogate data using stable distributions and then compare the values of RQA parameters.

If we apply RQA to shuffled surrogates, the RQA measures do not detect any structure giving for example *%determinism*, *%recurrence* and *%laminarity* equal to zero for all cases.

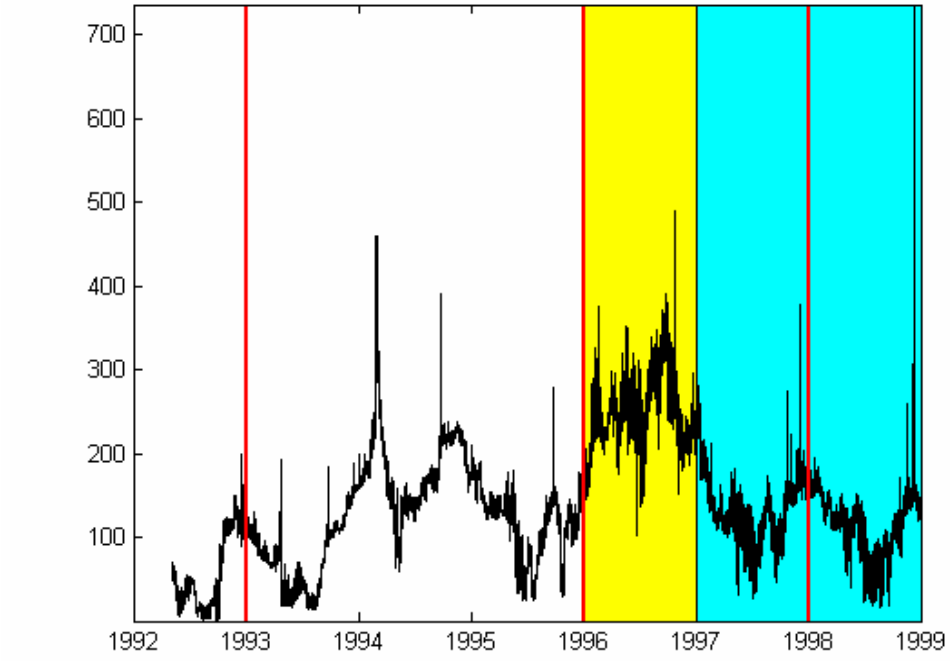

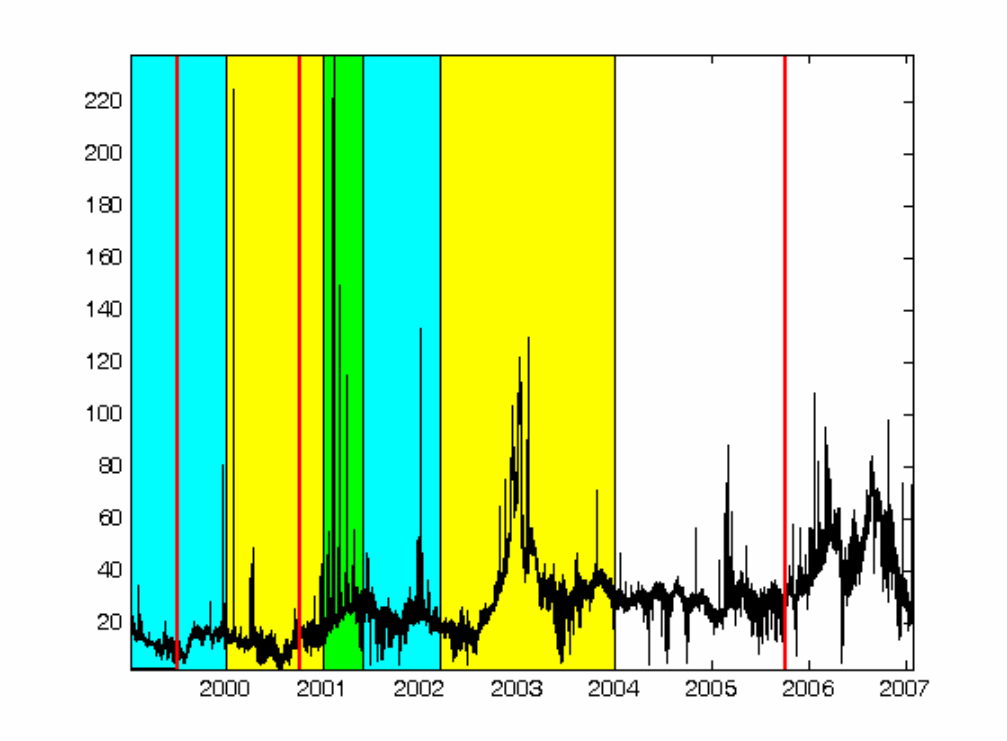

Figure 22. NOK/MWh (top) and EUR MWh (bottom) and the dates from Tables 1-3

4.5.4. RQE analysis

Let now compute RQA measures on a moving window. In this way, we obtain a time dependent profile of RQA measures. We would like to see if RQA measures are able to detect some events that are not clear from a direct inspection of the time series. For example we are interested to observe if some changes in the RQA parameters occur in correspondence of the entry of a new country in the Nord Pool (Table 1) or in correspondence with the starting of the deregulation processes (Table 2), or in correspondence with dry and wet years (Table 3). Figure 22 shows the two Nord Pool time series plotted with the dates or periods indicated in Tables 1-3, whereas in Figs. 23-24 the behaviour of RQA parameters is plotted with a moving window of one month shifted of one month for NOK/MWh and EUR/MWh, respectively.

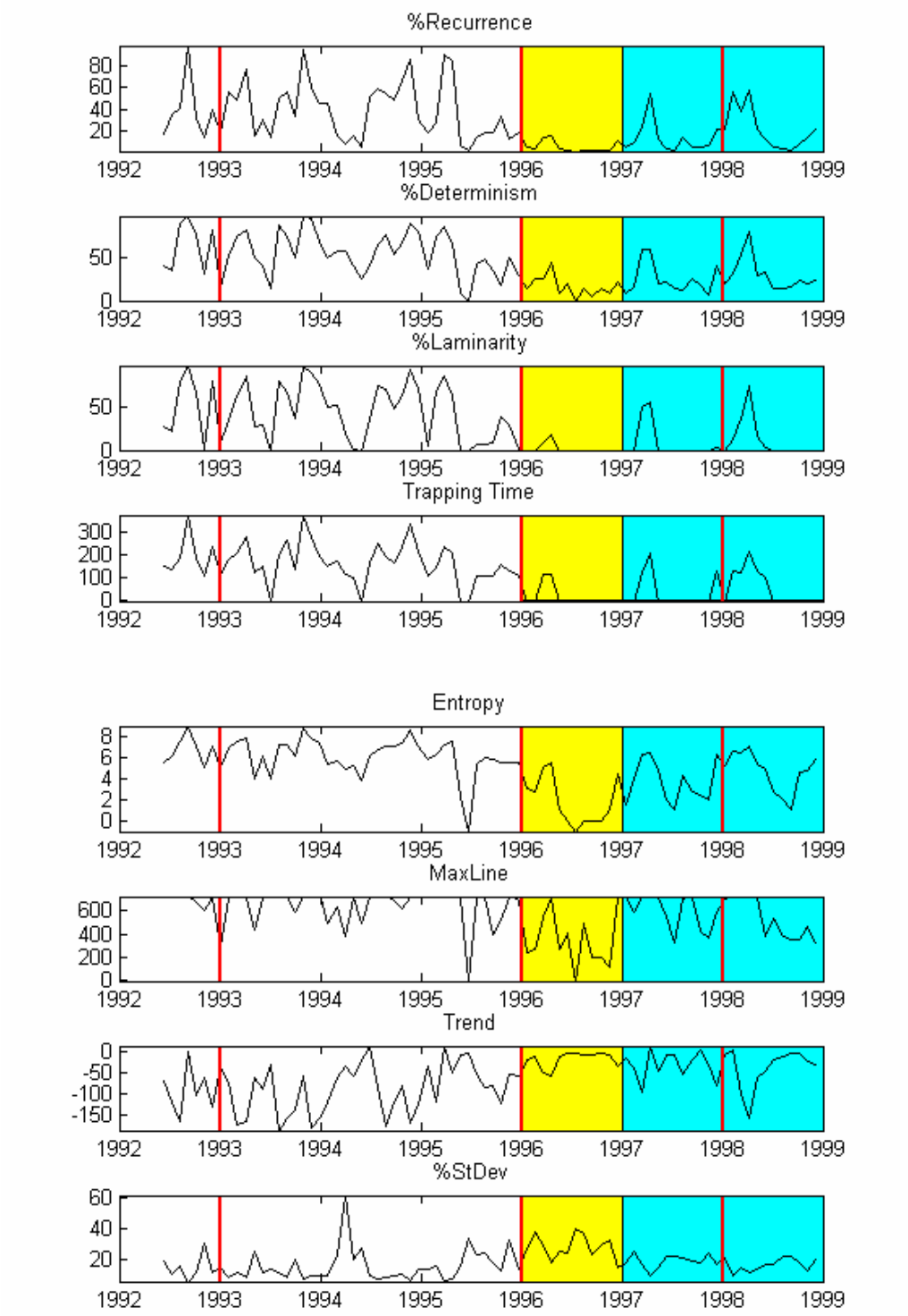

Figure 23. Nonlinear metrics of the Nord Pool spot prices time series in NOK/MWh: Values are computed from a 720 point window (one week), data are shifted 720 points. RQA parameters: τ =15, d_E=10, distance cutoff: max. distance between points/10, line definition: 100 points (~4 days). Vertical lines correspond to the following dates: 1st January 1993, 1st January 1996, 29th December 1997 and 1st July 1999 (see historical background).

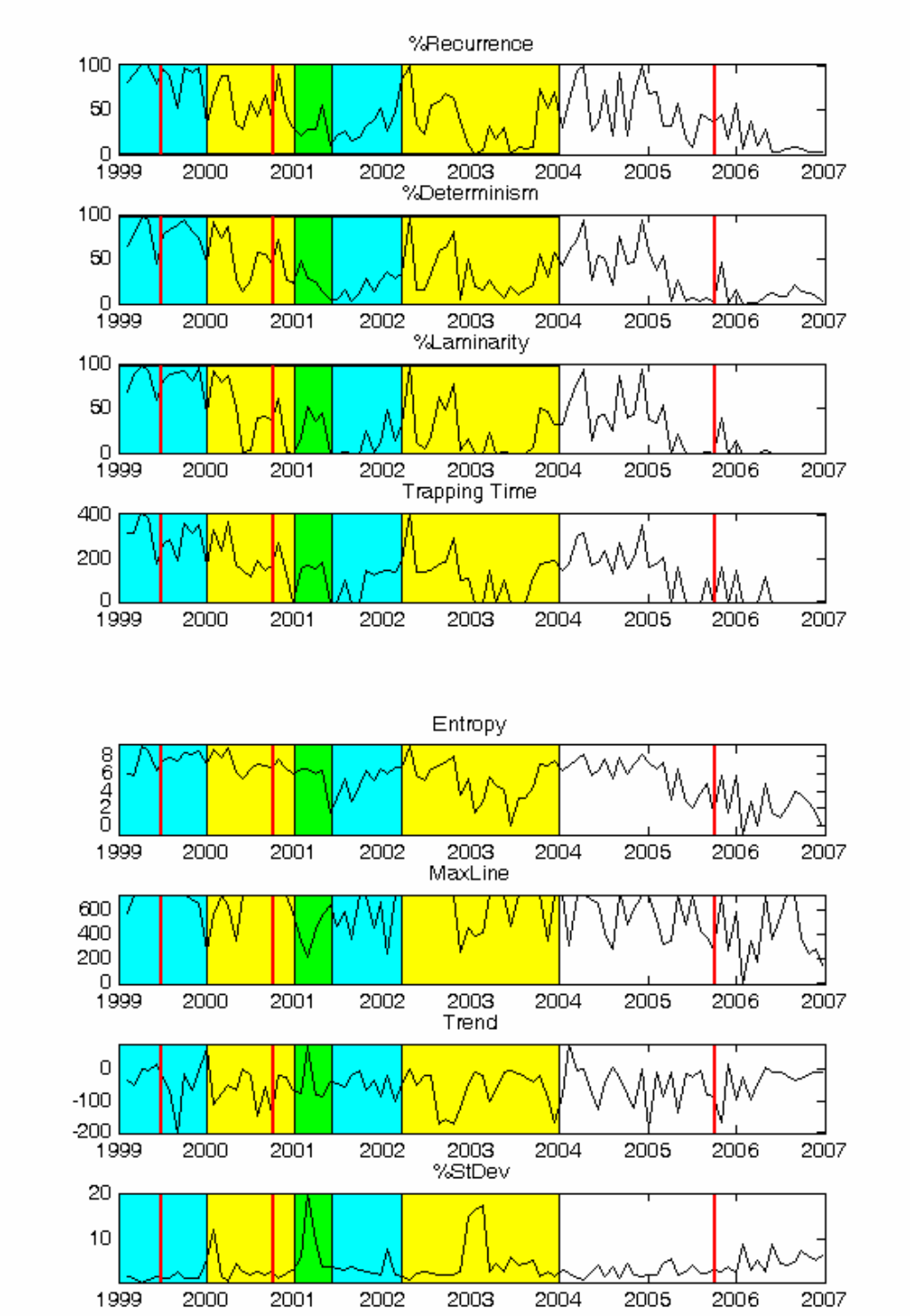

Figure 24. RQA measures of EUR/MWh: Values are computed from a 720 point window (one month), shifted of 720 points. RQA parameters: τ =13, d_E=10, distance cutoff: max. distance between points/10, line definition: 100 points (~4 days). Vertical lines correspond to the following dates: 1st October 2000, 5th October 2005 (see historical background).

By looking at Figs. 23-24 we can observe a qualitative agreement between the RQA measurements: *%recurrence*, *%determinism*, *%laminarity* and *trapping time,* for both time series. Furthermore, most of the times, it is possible to observe an inflection in correspondence of the entrance of a new state in Nord Pool (red

lines in Figs. 23 and 24 and Table 1). These lines also sometimes coincide with the starting of deregulation processes in other countries (see Table 2). However, there is no clear evidence and also inflections are visible in other parts of the time series.

In addition by looking at the RQA parameters (*%recurrence*, *%determinism*, *%laminarity* and *trapping time*) we can observe that, in correspondence of dry periods (yellow periods), the parameters tend to have smaller values and/or a negative trend. This is more clear in the first time series where hydroelectric power was more important for the Nord Pool. In these dry periods, due to the high dependence from the oil, the volatility of the price increases.

It is well-known that high volatility periods are those in which it is more difficult to make forecast. Higher *%determinism* and *%laminarity* mean that the states of the system stay closer in time for longer periods forming diagonal or vertical segments in RP. Then we can assume that higher *%determinism* or *%laminarity* implies smaller volatility. To study the relationship with volatility, we have compared the profiles of these quantities with the inverse of standard deviation between 0 and 100 (see figs. 25-26). The main difference between *%determinism* and *%laminarity* is that, in the periods of high volatility, *%laminarity* reaches zero values which gives a more clear signal of volatility periods.

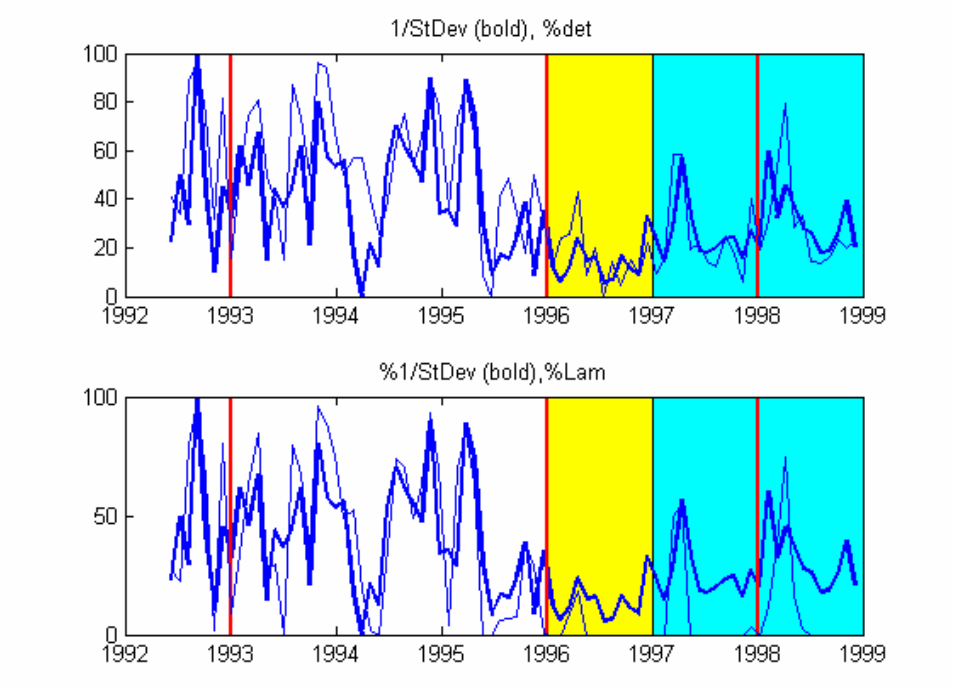

Figure 25. Inverse of standard deviation and *%determinism* (top) and *%laminarity* (bottom) for NOK/MWh

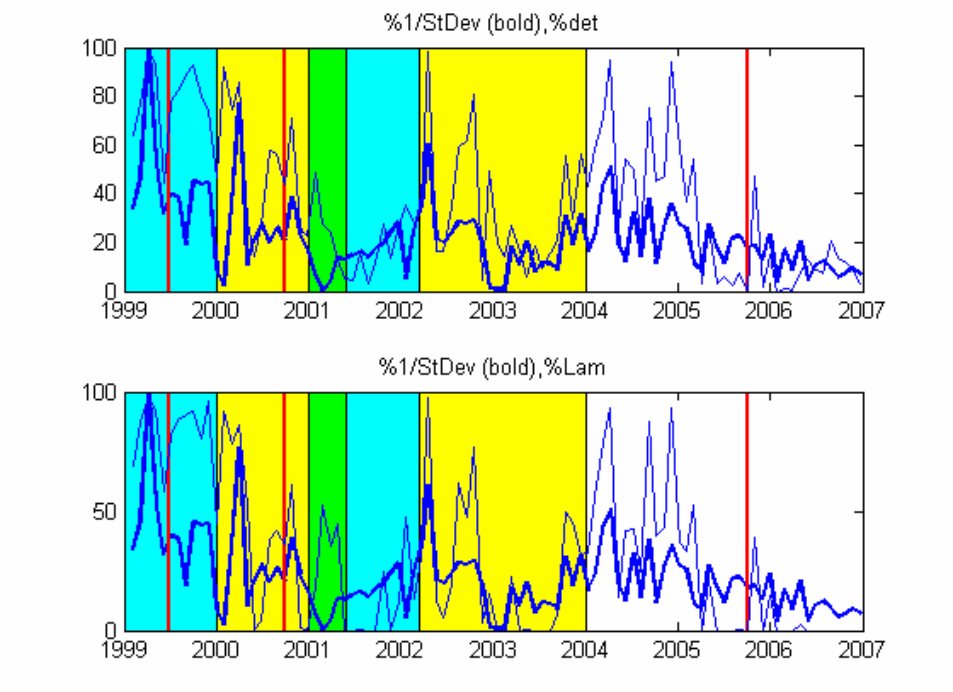

Figure 26. Inverse of standard deviation and *%determinism* (top) and *%laminarity* (bottom) for EUR/MWh

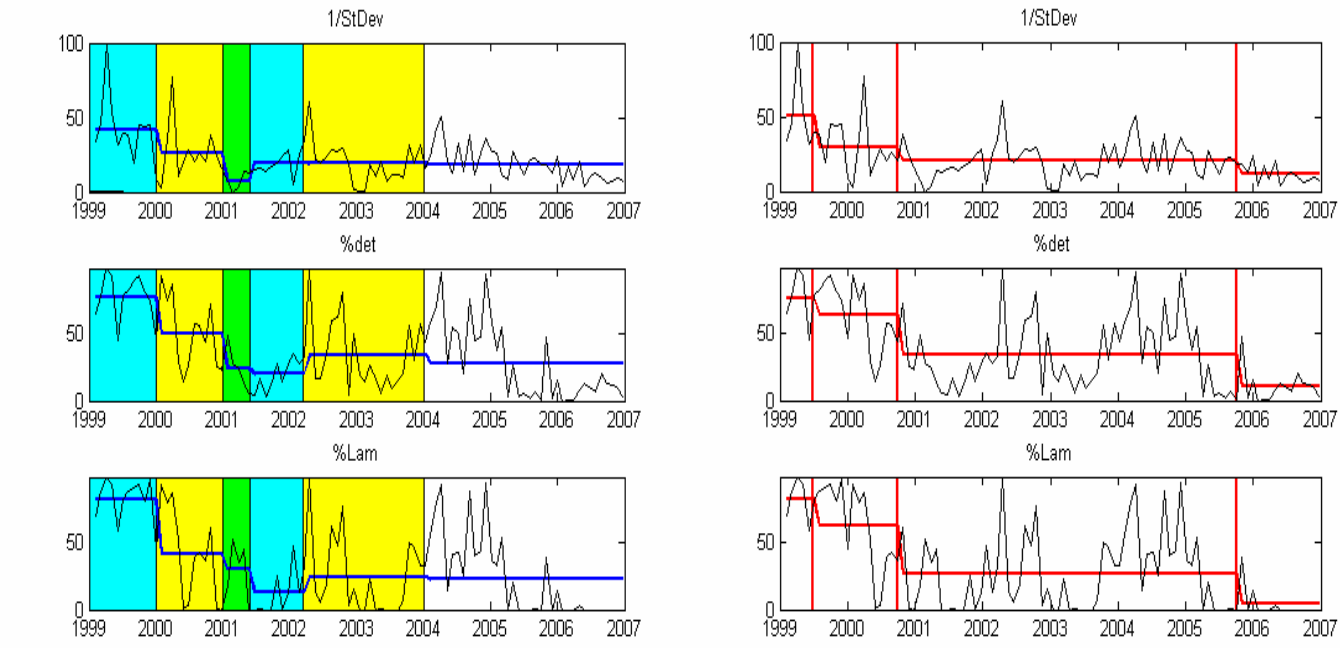

Figure 27. RQA measures of EUR/MWh: Values are computed from a 720 point window (one month), shifted of 720 points. RQA parameters: □=13, dE=10, distance cutoff: max. distance between points/10, line definition: 100 points (~4 days). Vertical lines correspond to the following dates: 1st October 2000, 5th October 2005 (see historical background).

In order to extract more information from RQA measures, we have compared the mean values of *%determinism* and *%laminarity* with the mean values of the inverse of the standard deviation (StDev) during the periods between changes in weather conditions (for EUR fig 27, left, and fig. 28 left for NOK) and the periods between the entrance of new states in Nord Pool (fig 27 right for EUR, fig 28 right for NOK). In both

cases, it is possible to observe that using RQA measures the changes in the means are more evident (the steps higher) than using standard deviation. Then using the RQA measures it is possible to improve the detection of changes in the time series analyzed.

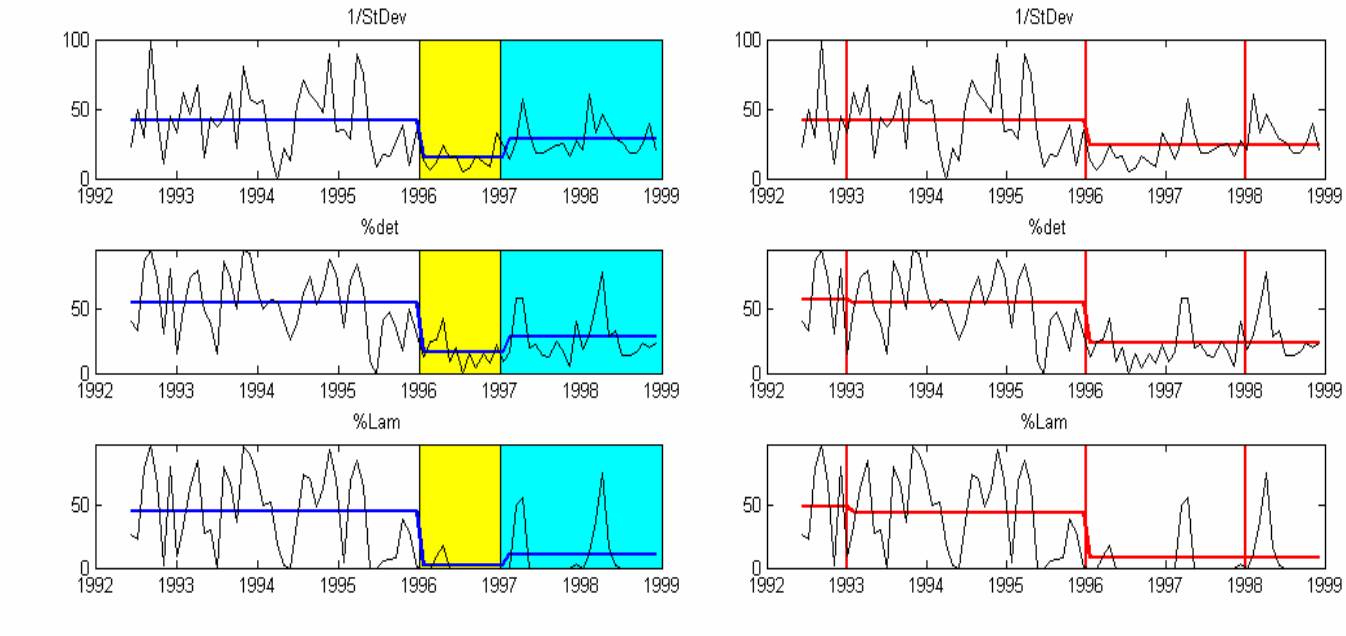

Figure 28. Nonlinear metrics of the Nord Pool spot prices time series in NOK/MWh: Values are computed from a 720 point window (one month), data are shifted 720 points. RQA parameters: τ =15, d_E=10, distance cutoff: max. distance between points/10, line definition: 100 points (~4 days). Vertical lines correspond to the following dates: 1st January 1993, 1st January 1996, 29th December 1997 and 1st July 1999 (see historical background).

5. Conclusions

Nonlinear time series analysis has been carried out for the Nord Pool time series. Preliminary analysis confirms already published work concerning the antipersistence, H<0.5, of these type of data sets. The power spectral density shows a scaling behaviour typical of financial time series. On the contrary, like in other high frequency time series such as exchange rates, the saturation in the space time separation plot shows that the time series may be considered as stationary and hence, the application of the surrogate data tests, that assumes two kinds of null hypothesis: stationary Gaussian linear process or no correlation at all, is adequate.

Stable distributions have been proposed as a model for many types of physical and economic systems because many large data sets exhibit heavy tails and skewness. It is possible to observe a clear distinction between the first period time series in NOK and the second in EUR. In the first case there is a considerable number of zeros in the first difference of the series that create some problems in fitting the parameters for a stable distribution, whereas the problem does not exist in the second case. In general terms the series seems to have long tails and be more similar to a Levy distribution than to a Gaussian one. Also in this case, linear surrogate data produce different values when fitted with stable distributions being more similar to a Gaussian (α =1.7 instead of 1.3) and having more symmetry, with β closer to 0 than their original series that have more skew.

The application of RQA shows some critical points in the series that loosely correspond with some historical periods; however it is difficult to assign a one to one correspondence. Also in this case some RQA measures are able to distinguish between linear and shuffled surrogates time series and the original ones. We have also found a correspondence between *%determinism* and *%laminarity* with the inverse of the standard deviation, therefore, these parameters can give another method to measure volatility in time series analysis. We have compared the mean values of these three quantities calculated between the periods in which there were important changes in weather conditions or in correspondence of which there was the incorporation of new states into the Nord Pool. We have shown that *%determinism* and *%laminarity* detect these changes more clearly than standard deviation and then they provide an alternative measure of volatility.

The future developments of this work will be to find a correlation between market prices (or some related variable such as volatility) and the likelihood of blackouts. In this work, candidate parameters have been assessed.

Acknowledgements. The authors gratefully acknowledge the financial support of the MANMADE NEST Project (Contract No 043363) and Dr. H. Sivonen (NESA) who kindly provided the data sets analysed.

References

Abarbanel, H.D.I., *Analysis of Observed Chaotic Data*, 1996, Springer-Verlag, New-York.

Amundsen, E.S. and Bergman, L., 2007, Integration of multiple national markets for electricity: The case of Norway and Sweden, *Energy Policy*, doi.1016/j.enpol.2006.12.014.

Andreadis, I., 2000, Self-criticality and stochasticity of an S&P 500 index time series. *Chaos, Solitons and Fractals* **11**, 1047-1059.

Badii, R., Broggi, G., Derighetti, B., Ravani, M., Ciliberto, S., Politi, A. and Rubio, M. A., 1988, Dimension increase in filtered signals. *Phys. Rev. Lett*. **60**, 979-982.

Bak, P. and Chen, K., 1991, Self-organized criticality. *Scientific American* **264**, 26-33.

Bask, M. Liu, T. and Widerberg, A., 2007. The stability of electricity prices: Estimation and inference of the Lyapunov exponents. *Physica A* **376,** 565-572.

Breeden, J. L and N. H. Packard, 1994, A learning algorithm for optimal representation of experimental data, *Int. J. of Bifurcations and Chaos* **4**, 311- 326.

Brock, W. A., Hsieh, D. A., LeBaron, B., 1991, *Nonlinear dynamics, chaos and instability: Statistical theory and Economic evidence*. MIT Press, Massachusetts, MA.

Broomhead, D. S. and G. P. King, 1986, Extracting qualitative dynamics from experimental data, *Physica D* **20**, 217-236.

Burden, R. L. and Faires, J. D. 1996. *Numerical Analysis* , 3rd Ed., PWS, Boston.

Byström H.N. E. 2005. Extreme value theory and extremely large electricity price changes. *International Review of Economics and Finance* **14**, 41-55.

Cannon, M. J. Percival, D. B., Caccia, D. C., Raymond, G. M. and Bassingthwaighte, J. B., 1997, Evaluating scaled windowed variance methods for estimating the Hurst coefficient of time series. *Physica A* **241**, 606-626.

Cao, L. ,1997, Practical method for determining the minimum embedding dimension of a scalar time series. *Physica D* **110**, 43-50.

Cao, L., 2002, Method of False Nearest Neighbors, in *Modelling and Forecasting Financial Data*, A. S. Soofi and L. Cao (Eds.), Kluwer, Boston.

Casdagli, M., Eubank, S., Farmer, J. D., Gibson, J., 1991, State space reconstruction in the presence of noise. *Physica D* **51**, 52-98.

Davies, M., 1994, Noise reduction schemes for chaotic time series, *Physica D* **79**, 174-192.

Diks, C., 1999, *Nonlinear Time Series Analysis: Methods and applications*.World Scientific, Singapore.

Eckmann, J. P., Kamphorst, S. O. and Ruelle, D., 1987, Recurrence plots of dynamical systems, *Europhys. Lett*. **4**, 973-977.

Farmer, J.D. and Sidorowich, J. 1987. Predicting chaotic time series. *Phys. Rev. Lett*. **59**, 845-850.

Fraser, A. and Swinney, H., 1986, Independent coordinates for strange attractors from mutual information. *Phys. Rev. A* **33**, 1134-1140.

Friederich, R., Peinke, J. and Renner, Ch., 2000, How to quantify deterministic and random influences on the statistics of the foreign exchange market. *Phys. Rev. Lett*. **84**, 5224-5227.

Gilmore, R., 1998, Topological analysis of chaotic dynamical systems. *Rev. Mod. Phys*. **70**, 1455-1529.

Grassberger, P., 1983, Generalized dimension of strange attractors. *Phys. Lett A* **97**, 227-230.

Haldrup, N., Nielsen, M. Ø., 2006. A regime switching long memory model for electricity prices. *Journal of econometrics* **135**, 349-376.

Hegger, R., Kantz, H., Schreiber, T., 1999, Practical implementation of nonlinear time series methods: The TISEAN package. *CHAOS* **9**, 413-. The software package is publicly available at http://www.mpipks-dresden.mpg.de/~tisean .

Hsieh, D. A., Chaos and nonlinear dynamics: Application to financial markets, 1991, *The Journal of Finance* **46**, 1839-1887

Hurst, H. E., 1951, Long-term storage capacity of reservoirs, *Trans. Am. Soc. Civ. Eng*. **116**, 770-779.

Johnson, N. F., Jefferies, P. & Ming Hui, P. 2003. *Financial Market Complexity*, Oxford University Press.

Kantz H., Shreiber T., 1997. *Nonlinear Time Series Analysis*, Cambridge University Press

Kennel, M. B., R. Brown and H. D. I. Abarbanel, 1992. Determining embedding dimension for phase-space reconstruction using a geometrical construction. *Phys. Rev. A* **45**, 3403-3411.

Koebbe, M., Mayer-Kress, G. 1992. Use of recurrence plots in the analysis of time-series data, in M. Casdagli, S. Eubank (Eds.). Proceedings of SFI Studies in the Science of Complexity, vol. XXI, Redwood City, Adison-Wesley, Reading, MA, pp. 361-378.

Kostelich, E. J. and Schreiber,T., 1993, Noise reduction in chaotic time-series data: A survey of common methods. *Phys. Rev. E* **48**, 1752-1763.

Kristiansen, T., 2006, A preliminary assessment of the market coupling arrangement on the Kontek cable, *Energy Policy* (in press)

Kristiansen, T., 2007. Pricing of monthly contracts in the Nord Pool market. *Energy Policy* **35**, 307-316.

Lorenz, H. W., 1993, *Nonlinear dynamical economics and chaotic motion*. Springer, New York.

Malkiel, B., 1990, *A random walk down Wall Street*, Norton, New York.

Mandelbrot, B. B., 1998, *Fractals and Scaling in Finance: Discontinuity, Concentration, Risk*. Springer, New York.

Mandelbrot, B. B., *The Fractal Geometry of Nature*, 1983, W. H. Freeman. New York.

Mantegna, R. N. & Stanley, H. E., 2000. *An introduction to Econophysics*. Cambridge University Press.

Mantegna, R. N. and Stanley, H.E., 1995, Scaling behaviour in the dynamics of an economic index. *Nature* **376**, 46-49.

Mantegna, R. N. and Stanley, H.E., 1996, Turbulence and financial markets. *Nature* **376**, 46-49.

Marwan, N., Romano, M. C., Thiel, M. and Kurths, J., 2007. Recurrence plots for the analysis of complex systems. *Physics Reports* **438**, 237-329.

Marwan, N., Wessel, N., Meyerfeldt, U., Schirdewan, A., Kurths, J. 2002. Recurrence plot based measures of complexity and its application to heart rate variability data. *Phys. Rev. E* **66**(2), 026702.

Mees, A. I., Rapp, P. E. and Jennings L. S., 1987, Singular value decomposition and embedding dimension. *Phys. Rev. A* **36**, 340.

Mork, E. 2001. Emergence of financial markets for electricity: a European perspective. *Energy Policy* **29**, 7-15.

Nolan, J.P., 1997. Numerical computation of stable densities and distribution functions. *Commun. Stat.: Stochastic models* **13**, 759-774.

Nolan, J.P., 1999. Fitting data and assessing goodness of fit with stable distributions. In *Proceedings of the Conference on Applications of Heavy Tailed Distributions in Economics, Engineering and Statistics*, American University, Washington DC, June 3-5.

Osborne, M. F.M., 1959, Brownian motion in the stock market. *Oper. Res*. **7**, 145-173.

Packard, N., Crutchfield, J., Farmer, D. and Shaw, R., 1981, Geometry from a time series. *Phys. Rev. Lett*. **45**, 712-715.

Papaioannou, G. and Karytinos, A., 1995, Nonlinear time series analysis of the stock exchange: The case of an emerging market. *Int. J. of Bifurcations and Chaos* **5**, 1557-1584.

Perelló, J., Montero, M., Palatella, L., Simonsen, I. and Masoliver, J., 2007. Entropy of the Nordic electricity market:anomalous scaling, spikes, and mean-reversion. *J. Stat. Physics* (in press).

Peters, E. E., 1996. *Chaos and Order in the Capital Markets: a New View of Cycles, Prices and Volatility*, 2nd Edition, Wiley, New York.

Provenzale, A., Smith, L. A., Vio, R. and Murante, G., 1992, Distinguishing between low-dimensional dynamics and randomness in measured time series. *Physica D* **58**, 31-49.

Ruelle, D., 1990, Deterministic chaos: the science and the fiction. *Proc. R. Soc. Lond. A* **427**, 241-248.

Scheinkman, J. and LeBaron, B., 1989, Nonlinear dynamics and stock returns. *J. Business* **62**, 311-318.

Schreiber, T. and Schmitz, A., 2000, Surrogate time series, *Physica D* **142**, 346-382.

Schreiber, T. and Schmitz, A.,1996, Improved surrogate data for nonlinearity tests. *Phys. Rev. Lett*. **77**, 35-38.

Schreiber, T., 1998, Interdisciplinary application of nonlinear time series methods. *Physics Reports*.

Shlesinger, M. F., Zaslavsky, G. M., and Klafter, J., 1993, Strange kinetics. *Nature* **363**, 31-37.

Simonsen, I., 2003. Measuring anti-correlations in the Nordic electricity spot market by wavelets. *Physica A* **322**, 597-606.

Soofi, A. S. and Cao, L:, 2002. *Modelling and forecasting financial data: Techniques of Nonlinear Dynamics.* Kluwer Academic Publishers, Norwell.

Stark, J., Broomhead, D.S., Davies, M.E. and Huke, J.1997, Takens embedding theorems for forced and stochastic systems. *Nonlinear Analysis* **30**, 5303-5314.

Strozzi, F. and Zaldívar, J. M., 2002, Embedding theory: Introduction and applications to time series analysis, in *Modelling and forecasting financial data: Techniques of Nonlinear Dynamics*. A. Soofi and L. Cao (Eds.), Kluwer Academic Publishers, Boston.

Strozzi, F., Zaldívar, J, M., Zbilut, J., P., 2007, Recurrence quantification analysis and state space divergence reconstruction for financial time series analysis. *Physica A* **376**, 487-499

Strozzi, F., Zaldívar, J. M., & Zbilut, J. P. 2002. Application of nonlinear time series analysis techniques to high frequency currency exchange data, *Physica A* **312**, 520-538.

Takens, F., 1981, in Dynamical Systems and Turbulence, Warwick 1980, vol. 898 of Lecture Notes in Mathematics, edited by A. Rand and L.S Young, Springer, Berlin, pp. 366-381.

Takens, F., 1996, The effect of small noise on systems with chaotic dynamics. In *Stochastic and Spatial Structures of Dynamical Systems*, S. J. van Strien and S. M. Verduyn Lunel, Verhandelingen KNAW, Afd. Natuurkunde, vol. 45, pp. 3-15. North-Holland, Amsterdam.

Theiler, J., 1991, Some comments on the correlation dimension of $1/f^{\alpha}$ noise. *Phys. Lett A* 155, 480-493.

Theiler, J., Eubank, S., Longtin, A., Galdrikian, B., and Farmer, J. D., 1992, Testing for nonlinearity in time series: the method of surrogate data. *Physica D* **58**, 77-.

Thiel, M., Romano, M.C., Kurths, J., Meucci, R., Allaria, E. and Arecchi, F.T. 2002. Influence of observational noise on the recurrence quantification analysis. *Physica D* **171**, 138-152.

Tong, H., *Nonlinear Time Series: a Dynamical System Approach*. 1990, Oxford University Press. Oxford.

Trulla, L.L, A. Giuliani, J.P. Zbilut, and C.L. Webber, Jr. 1996. Recurrence quantification analysis of the logistic equation with transients. *Phys. Lett. A* **223**, 255-26.

Vehviläinen I. and Pyykkönen, T. 2005. Stochastic factor model for electricity spot price-the case of the Nordic market. *Energy Economics* **27**, 351-357.

Webber Jr. C. L. and Zbilut, J. P., 1994. Dynamical assessment of physiological systems and states using recurrence plot strategies. *J. Appl. Physiol*. **76**, 965-973.

Weron, R. and Przybyłowicz, B., 2000. Hurst analysis of electricity price dynamics. *Physica A* **283**, 462-468.

Weron, R., Bierbrauer, M. and Truck, S. 2004. Modelling electricity prices: Jump diffusion and regime switching. *Physica A* **336**, 39-48.

Whitney, H., 1936. Differentiable manifolds. *Ann. Math.* **37**, 645-680.

Wolf A., J. B. Swift, H. R. Swinne, J. A. Vastan, 1985. Determining Lyapunov exponents from a time series, *Physica D* **16**, 285-317.

Zaldívar, J.M., Strozzi, F., Dueri, S., Marinov, D. and Zbilut, J. P. 2007. Recurrence quantification analysis as a method for the detection of environmental thresholds. *Ecol. Model.* (in press)

Zbilut, J. P. and Webber Jr. C. L., 1992. Embeddings and delays as derived from quantification of recurrence plots. *Phys. Lett. A* **171**, 199-203

Zbilut, J. P., Zaldívar, J. M., Strozzi, F., 2002. Recurrence quantification based Liapunov exponents for monitoring divergence in experimental data. *Phys. Lett. A* **297**, 173-181.